JOC The Journal of Organic Chemistry

Article

pubs.acs.org/joc

# Self-Assembly of Hekates-Tris(*N*-salicylideneaniline)s into Columnar Structures: Synthesis and Characterization

Ammathnadu S. Achalkumar,[†] Uma S. Hiremath, D. S. Shankar Rao, S. Krishna Prasad, and Channabasaveshwar V. Yelamaggad*

Centre for Soft Matter Research, Jalahalli, Bangalore, 560 013, India

Supporting Information

**ABSTRACT:** Two series of new, photoluminescent star-shaped discotic liquid crystals, recently termed as "hekates", derived from tris(*N*-salicylideneaniline)s (TSANs), were synthesized by the facile threefold condensation of 3,4-bis(alkoxy)phenyl 4-aminobenzoates/3,4,5-tris(alkoxy) phenyl 4-aminobenzoates with 1,3,5-triformylphloroglucinol and characterized. These two series of discotics with six and nine peripheral *n*-alkoxy tails were especially designed and accomplished to understand the relation between mesomorphic/photophysical properties and molecular structure. Proton NMR spectral analysis revealed their existence as an inseparable mixture of two keto-enamine tautomeric forms featuring $C_{3h}$ and $C_s$ rotational symmetries. A systematic study into the thermotropic liquid crystal behavior using polarizing optical microscopy, differential scanning calorimetry, and X-ray scattering confirmed the presence of columnar (Col) phase in vast majority of the TSANs prepared. The two-dimensional (2D) lattices of these fluid columnar phases were found to be characteristic of hexagonal Col ($Col_h$), rectangular Col ($Col_r$), or oblique Col ($Col_{ob}$) phases depending on the number/length of the peripheral flexible chains. The stabilization of the $Col_{ob}$ phase, a less commonly found fluid columnar structure, and the first of its kind in TSAN systems, implies very intensive intermolecular (face-to-face) interactions among the TSAN cores within the column. The photophysical properties were investigated both in solution and the columnar states by UV−vis absorption and photoluminescence; markedly, the solution state emits light in the blue region. The light-emitting ability of the Col phase is particularly significant given the possibility that, in such cores, the protons and electrons interact with each other through the H-bonding environment.

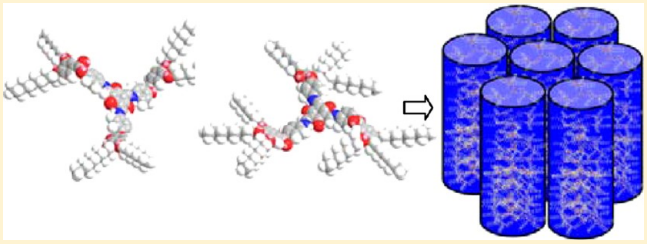

## INTRODUCTION

The $\pi$-conjugated organic materials capable of facilitating one-dimensional (1D) charge transport have been attracting a great deal of attention owing to their potential promise for a wide range of electronic and optoelectronic devices.[1] In particular, there have been constant efforts in deriving high-quality single crystals from $\pi$-conjugated organic molecules as they provide a fine-tuned 1D molecular ordering through $\pi-\pi$ interactions, which is one of the key parameters required for the improved performance of electronic devices.[2,3] However, as is well-known, one of the major and inevitable problems associated with single crystals is the presence of defects that disrupts the charge migration significantly; further, the process of defect elimination in single crystals is rather difficult. On the other hand, discotic liquid crystals (LCs),[4] generally formed by disklike shape-anisotropic organic molecules, discovered by Chandrasekhar et al. in 1977,[5] have been regarded as one of possible substitutes[6] to zone refined single crystals. This is because the vast majority of discotics self-organize spontaneously into indefinitely long columnar stacks that are highly anisotropic and ordered structures with extensive $\pi$-orbital overlap leading to a high degree of uniaxial charge-carrier mobilities.[4,6,7] In fact, the measured mobility value in columnar (Col) LCs exceeds 1 $cm^2\ V^{-1}\ s^{-1}$.[8] Most importantly, they possess the ability of orientational control of the molecular order and eliminate structural/electronic defects effectively by self-healing process.[4,6] Besides, being fluid, they can be easily processed in various forms required for applications.

Hitherto, a large number of discotics have been designed and synthesized not only to realize Col LCs capable of exhibiting high charge-carrier mobilities but also to understand structure−property correlations.[4] The accumulated experimental results clearly indicate the importance of the chemical as well as electronic nature of the central core as it fundamentally determines the degree of order and $\pi-\pi$ molecular orbital overlap within the columnar stacks and thus the charge-carrier mobility of discotic LCs. In view of this, there have been numerous efforts in devising novel discotics derived from a new mesogenic core. For some time now, our group has been working in this direction, and an important result is the realization of an entirely new class of discotics occurring in the form of a mixture comprising two inseparable keto-enamine tautomers featuring $C_{3h}$ and $C_s$ rotational symmetries.[9] Indeed, we have as well reported supramolecular discotic TSANs existing in the exclusive $C_{3h}$ keto-enamine tautomeric form.[10]

**Received:** October 30, 2012
**Published:** December 6, 2012

**Chart 1. Molecular Structures of the Two Series of TSAN-based Hekates**

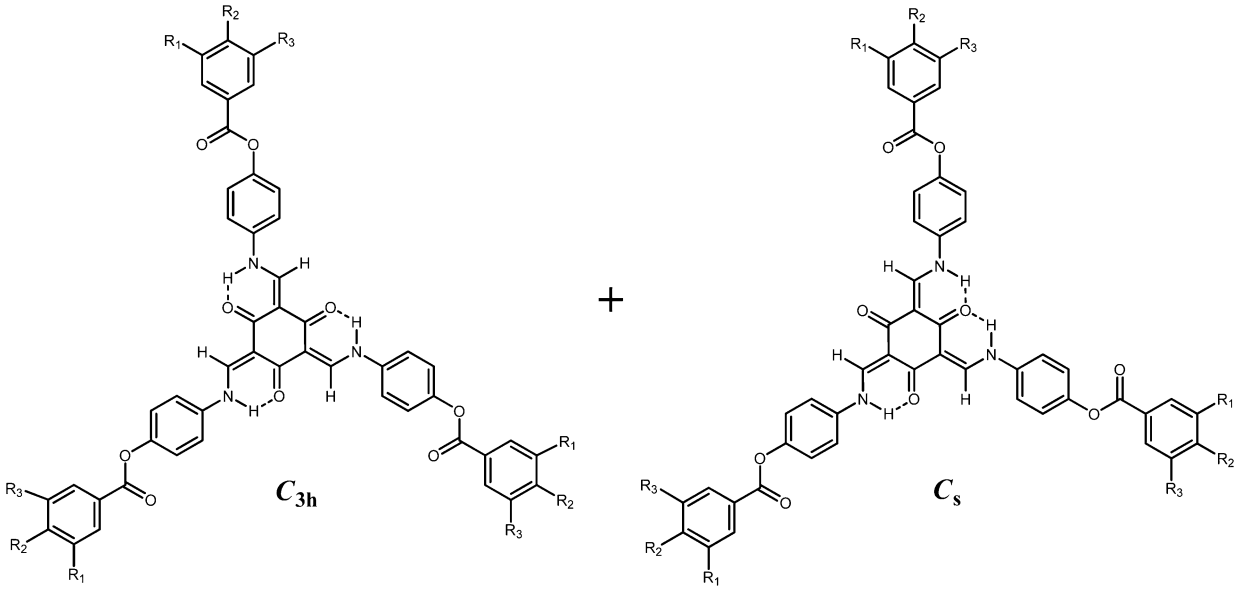


**Series I: DLT-n**

**DLT-6:** $R_1 = R_2 = OC_6H_{13}$, $R_3 = H$
**DLT-7:** $R_1 = R_2 = OC_7H_{15}$, $R_3 = H$
**DLT-8:** $R_1 = R_2 = OC_8H_{17}$, $R_3 = H$
**DLT-10:** $R_1 = R_2 = OC_{10}H_{21}$, $R_3 = H$
**DLT-12:** $R_1 = R_2 = OC_{12}H_{25}$, $R_3 = H$

**Series II: TLT-n**

**TLT-4:** $R_1 = R_2 = R_3 = OC_4H_9$
**TLT-5:** $R_1 = R_2 = R_3 = OC_5H_{11}$
**TLT-6:** $R_1 = R_2 = R_3 = OC_6H_{13}$
**TLT-7:** $R_1 = R_2 = R_3 = OC_7H_{15}$
**TLT-8:** $R_1 = R_2 = R_3 = OC_8H_{17}$
**TLT-10:** $R_1 = R_2 = R_3 = OC_{10}H_{21}$

These discotics are unique as they are derived from tris(*N*-salicylideneaniline) (TSAN) core that readily offers the possibility of inducing/tuning both smart material and electronic properties through appropriate molecular design.[11,12] In continuation of our studies in this area, we have rationally designed and prepared novel star-shaped TSANs where three extended (long) arms, in the form of phenyl benzoate substituted with six/nine peripheral *n*-alkoxy tails, have been covalently linked to the central cyclohexane-1,3,5-trione core.

The design of the present two series of TSANs stemmed from the fact that star-shaped LCs, recently referred to as "hekates",[13,14] which are formed by covalently joining three long mesogenic segments (arms) to a trifunctional central core through linking groups, have been attracting attention owing to their very promising features in the fields of both basic and applied sciences. Their self-organization into a functional columnar phase, for instance, has generated an adequate amount of basic curiosity as they possess rigid /semiflexible long arms directing radially away from the center and thus creating large voids.[13] This means that these shape-persistent motifs seriously lacking in conformational freedom find it difficult to account concurrently for both nanophase segregation and space-filling processes needed for the formation of the Col LC phase. In the context of practical applications, the hekates have been examined for their alignment (homeotropic or planar orientation) abilities,[16,17] plastic electronic materials characteristics,[4a,b,13,18] fast charge carrier mobility,[18] NLO phenomenon,[19] gelation ability,[20] luminescence behavior,[15,16,20,21] and so forth; besides, they have been also tested for their suitability in field effect transistor (FET) device application.[22] Considering these special aspects, we intended to realize new hekates derived from TSANs. The molecular structures of two series of accomplished TSANs are shown in their $C_{3h}$ and $C_s$ keto-enamine tautomeric forms in Chart 1. As can be seen, hekates TSANs realized comprise three semiflexible benzoate arms and a shape-persistent cyclohexane-1,3,5-trione core that are not only linked covalently but also associated with each other through intramolecular H bonding. The acronym used to describe the compounds of series I is **DLT-*n*** where **DLT** refers to **d**ialkoxy **l**ong-armed **T**SANs and ***n*** indicates the number of carbon atoms in the peripheral alkoxy chains. Whereas, materials of series II are denoted by the mnemonic **TLT-*n*** where **TLT** denotes **t**rialkoxy **l**ong-armed **T**SANs and ***n*** implies the length of the terminal tails.

## RESULTS AND DISCUSSION

**Synthesis and Characterization.** Two series of star-shaped TSANs were prepared following the synthetic strategies shown in Scheme 1. We first describe the synthesis of mesogens belonging to the **DLT-*n*** series where six *n*-alkoxy tails are attached at the periphery. 3,4-Dihydroxybenzaldehyde was O-alkylated with the appropriate 1-bromoalkane using a mild base to obtain 3,4-bis(*n*-alkoxy)benzaldehydes (**1a**–**e**),[23a–c] which upon subjecting to oxidation using Jones reagent[23c] yielded 3,4-bis(*n*-alkoxy)benzoic acids (**2a**–**e**).[23b] DCC-mediated esterification of the resultant carboxylic acids **2a**–**e** with 4-nitrophenol furnished 3,4-bis(*n*-alkoxy)phenyl 4-nitrobenzoates (**3a**–**e**), which on catalytic hydrogenation gave 3,4-bis(*n*-alkoxy)phenyl 4-aminobenzoates (**4a**–**e**). In the final step, anilines **4a**–**e** were condensed with 1,3,5-triformylphloroglucinol to obtain the **DLT-*n*** series of compounds in reasonably


dx.doi.org/10.1021/jo302332u | J. Org. Chem. 2013, 78, 527–544

**Scheme 1.** [a]

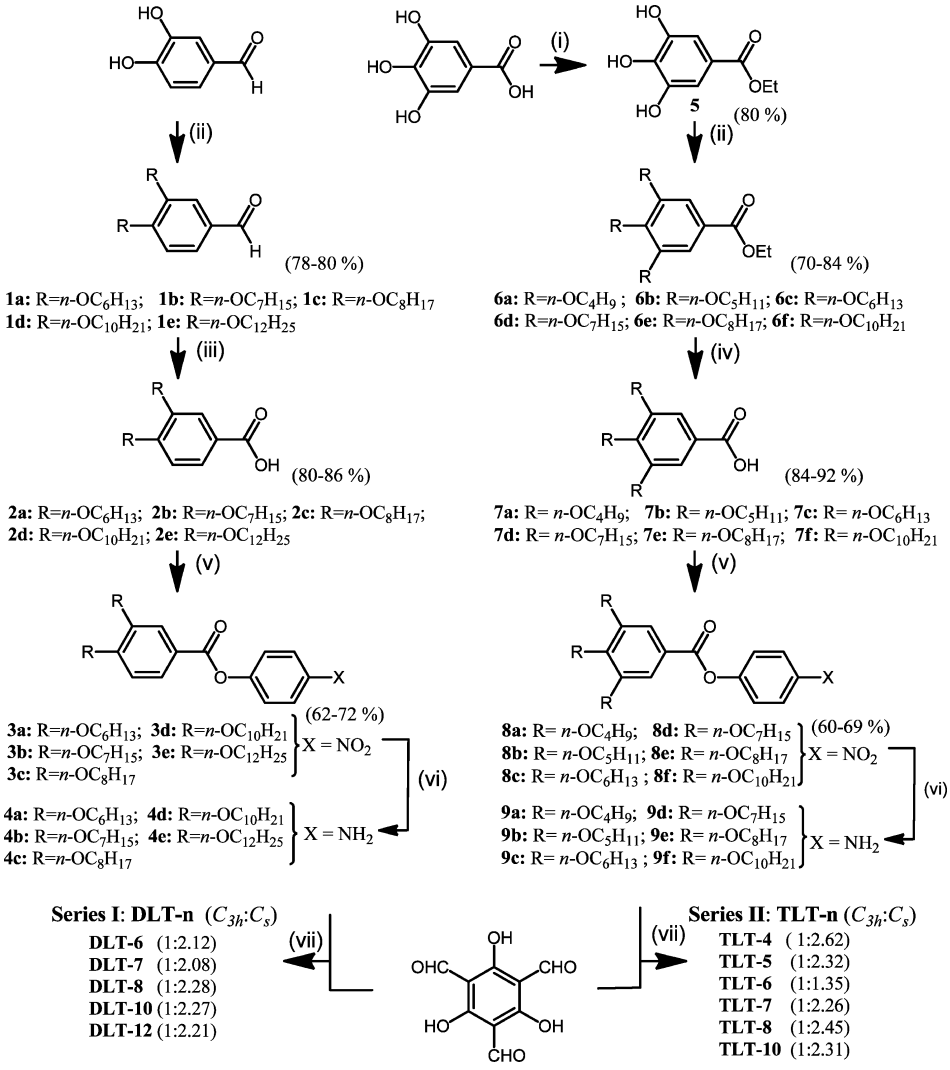


[a]Reagents and conditions: (i) Ethanol, conc $H_2SO_4$, reflux, 5 h. (ii) 1-Bromoalkane, anhyd $K_2CO_3$, DMF, 80 °C, 12 h, under $N_2$. (iii) Jones reagent, acetone, room temperature (RT), 1 h. (iv) 15% NaOH (aq), ethanol, reflux, 6 h. (v) 4-Nitrophenol, DCC, DMAP, THF, RT, 12 h. (vi) $H_2$ (1 atm, balloon), 10% Pd–C, THF, RT, 2 h. (vii) Ethanol, reflux, 2 h.

good yields. Hekates of the **TLT-n** series comprising nine peripheral alkoxy tails were realized starting from commercially available gallic acid. It was esterified with ethanol to obtain ethyl 3,4,5-trihydroxybenzoate (**5**), which on O-alkylation with the appropriate 1-bromoalkane using anhydrous potassium carbonate afforded the ethyl 3,4,5-trialkoxybenzoates (**6a–f**).[24] Saponification of ethyl gallates **6a–f** followed by acidification yielded 3,4,5-trialkoxybenzoic acids (**7a–f**),[25] which upon esterification with 4-nitrophenol in the presence of DCC furnished 3,4,5-tris(alkoxy)phenyl 4-nitrobenzoates (**8a–f**). Catalytic hydrogenation of these nitro precursors yielded 3,4,5-tris(alkoxy)phenyl 4-aminobenzoates (**9a–f**). Finally, anilines **9a–f** were condensed with 1,3,5-triformylphloroglucinol to obtain the target **TLT-n** series of compounds. The molecular structures of both intermediates and final compounds were established by standard spectroscopic and elemental analyses (see the Experimental Section as well as the Supporting Information for details).

The $^1$H NMR spectra of both the **DLT-*n*** and **TLT-*n*** series of hekates-TSANs displayed complex patterns in the regions $\delta$ 8.71–8.85 and 13–13.8 corresponding to two geometrical isomers having $C_{3h}$ and $C_s$ symmetries (Chart 1). The region $\delta$ 8.6–8.8 comprised three doublets, varying in their relative intensities, arising due to the resonance of an enamine (vinylic) proton of the $C_{3h}$ isomer and three analogous protons of the $C_s$ isomer. The region $\delta$ 13–13.8 consisted of multiple peaks, in the form of either three doublets or merged two doublets and a doublet differing in their relative intensities, originating because of the resonance of an amine proton of the $C_{3h}$ isomer and three protons of the $C_s$ form. It may be noted here that the short-armed TSANs reported earlier show four–four distinct doublets for amine–enamine protons.[9] Two-dimensional (2D) $^1$H–$^1$H correlation spectroscopy (COSY) NMR experiments showed the coupling between vinylic and NH protons. As illustrated in Scheme 1, the two geometrical isomers of both series I and II of TSANs were found to present in the ratio of 1:2 ($C_{3h}/C_s$). Most importantly, our studies clearly suggest the ratio of the two isomers is independent of the concentration of TSANs dissolved in $CDCl_3$. It may be noted here that, while assigning the ratio of two geometric forms, only the area under the peaks of amine protons have been considered because of the close proximity of chemical shifts of enamine protons. In


dx.doi.org/10.1021/jo302332u | J. Org. Chem. 2013, 78, 527–544

the $^{13}C$ spectra, all TSANs showed three characteristic signals at approximately $\delta$ = 188.2, 185.4, and 182.4 instead of expected four signals due to carbonyl carbons of the two isomers of the central cyclohexane-1,3,5-trione core. Likewise, the expected signals, especially in the downfield region from the residual $CHCl_3$ signals (a 1:1:1 triplet at $\delta$ = 77) arising due to two isomers could not be observed for any of the TSANs. This can be interpreted in terms of the fortuitous overlap of peaks as the two structures resemble each other closely.

**Evaluation of LC Behavior.** The thermal and mesomorphic properties of the synthesized hekates-TSANs were established with the aid of polarizing optical microscopy (POM), differential scanning calorimetry (DSC), and X-ray diffraction (XRD). An untreated glass slide and a coverslip were used for the examination of the LC property, the characteristic mobility (fluidity), and optical birefringence of the compounds using POM. A calorimetric (DSC) study complemented the phase transition temperatures noted during the optical study. The analysis of the results, to be described in the following sections, reveals the optimal diameter of the hard core and lengths of alkoxy tails required and the delicate balance of these parameters in stabilizing LC phases.

*Mesomorphic Behavior of the* ***DLT-n*** *Series.* Table 1 presents the phase sequences, transition temperatures, and associated enthalpies of the **DLT-*n*** series of hekates-TSANs derived from the aforementioned complementary studies. The thermal parameters are taken from the first heating−cooling cycles of DSC scans. The first member of the series, **DLT-6** with hexyloxy chains, was found to be nonmesomorphic. It melted directly into the isotropic liquid state at 130 °C, and on cooling, the sample crystallizes. Further increase in chain lengths results in an enantiotropic mesomorphism; while **DLT-7** and **DLT-8** display a single enantiotropic Col phase, higher homologues, namely, **DLT-10** and **DLT-12**, stabilize a bimesomorphic sequence involving a transition from one Col phase to the other. It may be mentioned here that TSAN with the *n*-nonyloxy tail (**DLT-9**) could not be obtained in pure form despite several attempts and hence was not reported. The occurrence of the Col phase was first ascertained by textural observations; for example, compound **DLT-12** placed between either clean glass slides or treated for planar or homeotropic geometry and cooled slowly from the isotropic phase shows a mesophase having a combination of pseudo-focal conic fan-shaped defects and homeotropic regions (Figure 1a), which is diagnostic for the presence of the Col phase; notably, as can be seen in the highlighted region of Figure 1a, on top of the focal conic fan-shaped patterns, very fine lines exist. On cooling these samples below this phase, a transition to another Col phase occurs with a prominent change in the texture, where as shown in Figure 1b, the fine lines over fan-shaped defects disappear. The DSC thermograms obtained during the first heating and cooling cycles shown in Figure 1c corroborate these observations. Notably, this Col phase gets into a glassy state as revealed by both optical and calorimetric studies. As summarized in Table 1, compound **DLT-10** showed a comparable behavior with an exception that it crystallizes while cooling from the low temperature columnar phase.

Powder XRD measurements were carried out to determine the symmetry of the thermodynamically stable Col phase formed by compounds **DLT-8**, **DLT-10**, and **DLT-12**. The diffraction patterns obtained in the Col phases of **DLT-8**, **DLT-10**, and **DLT-12** are shown in Figure 2a, 2b, and 2c, respectively. The results of indexing the sharp reflections in these profiles to lattices of a columnar phase are summarized in Table 2. The diffractogram obtained for the Col phase of **DLT-8** at 140 °C (Figure 2a) comprised three sharp reflections in the low-angle region ($0 < 2\theta < 9°$) with *d* spacings of 34.4, 17.1, and 12.9 Å. These values are in the ratio $1:1/\sqrt{4}:1/\sqrt{7}$, conforming to that expected for a hexagonal lattice (but for the missing $1/\sqrt{3}$ reflection) and indexed as (100), (200), and (3−10) diffractions of a hexagonal columnar ($Col_h$) assembly with an intercolumnar distance (*a*) of about 39.7 Å. Seemingly, the intercolumnar spacing is significantly smaller than 46.8 Å determined as the energy minimized (all-*trans*) diameter of the **DLT-8** (Figure 3a) through a chemdraw software. This disparity can be indeed interpreted by considering the molecular conformation/geometry of each discotic molecule within the column where the peripheral tails, being in the molten state, fold up to fill the voids. At high angles ($2\theta \approx 20°$),

**Table 1. Phase Transition Temperatures[a] (°C) and Corresponding Enthalpies (kJ/mol) of the DLT-*n* Series of Compounds[b]**

| compd DLT-*n* | phase sequence | |
|---|---|---|
| | heating | cooling |
| **DLT-6** | Cr 129.3 [7.7] I | I 104 [3.4] Cr |
| **DLT-7** | $Cr_1$ 109.1 [3.9] $Col_h$ 147.6 [1.8] I | I 143.2 [1.8] $Col_h$ 97.9 [2.5] Cr |
| **DLT-8** | Cr 124.1 [5.6] $Col_h$156.1 [1.9] I | I 151 [1.9] $Col_h$ 116.6 [5.6] Cr |
| **DLT-10** | Cr 77.4 [0.9] $Col_r$ 130.4 [7.2] $Col_h$ 169.6 [3.8] I | I 166.7 [3.6] $Col_h$ 116.8 [4.9] $Col_r$ 56.1 [11.4] Cr |
| **DLT-12** | Cr 69.4 [64.5] $Col_r$ 120.2 [2.3] $Col_h$ 170.7 [3.4] I | I 168.4 [3.2] $Col_h$ 114.9 [2.3] $Col_r$[c] |

[a]Peak temperatures in the DSC thermograms obtained during the first heating−cooling cycles at 5 °C/min. [b]Cr, $Cr_1$ = crystal; $Col_h$ = hexagonal columnar phase; $Col_r$ = rectangular columnar phase; I = isotropic liquid state. [c]The Col phase did not crystallize upon cooling down to −60 °C.

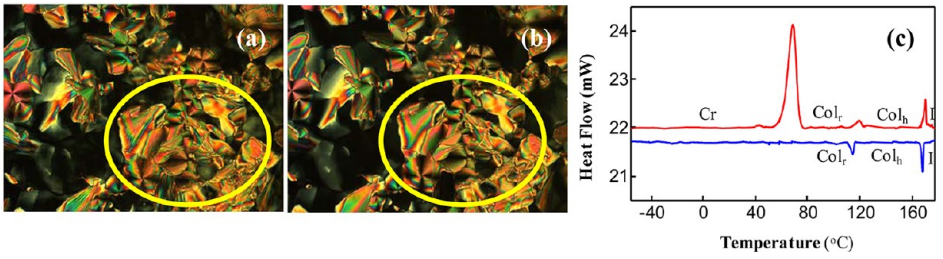


**Figure 1.** Photomicrographs of textures as seen by POM for the (a) $Col_h$ phase at 152 °C and (b) $Col_r$ phase at 108 °C of the compound **DLT-12**. (c) DSC traces obtained for the first heating (upper trace) and cooling (lower trace) cycles of **DLT-12** at a rate of 5 °C $min^{-1}$.


dx.doi.org/10.1021/jo302332u | J. Org. Chem. 2013, 78, 527−544

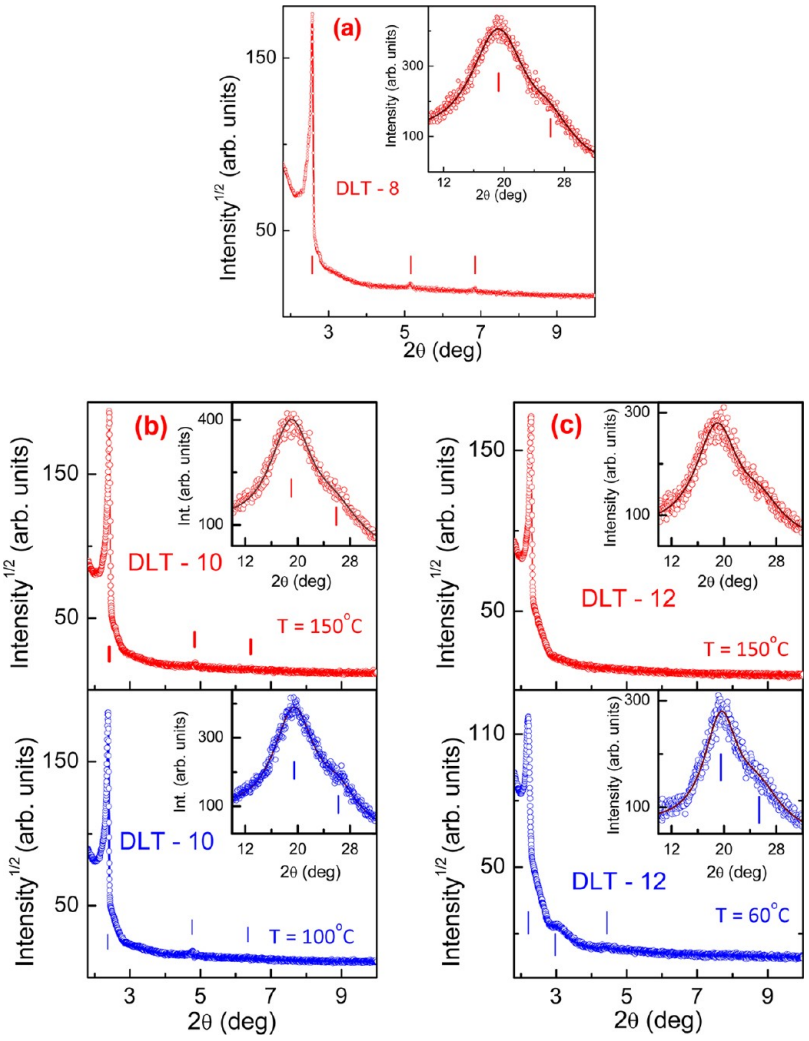


**Figure 2.** XRD profiles depicting the intensity against the $2\theta$ obtained for the Col phase(s) of compounds (a) **DLT-8**, (b) **DLT-10**, and (c) **DLT-12**. The insets show the diffuse profile in the wide-angle region that could be fit (solid line) to two Lorentzian peaks arising from short-range correlations between the alkyl chains (labeled $h_a$), and between the cores ($h_c$) within a single column. Note that peak positions are indicated by solid lines.

the sample showed two diffuse scattering maxima corresponding to distances of 4.6 and 3.4 Å that relate to a short-range correlation between the conformationally disordered alkoxy tails and the stacking distance of hekates-TSANs within the same column, respectively. In view of the foregoing discussions, we consider the mesophase stabilized by **DLT-8** to be the $Col_h$ phase. The schematic representation of the $Col_h$ phase, wherein local packing of the columns is hexagonal along the columnar axes, formed by the stacking of TSANs is shown in Figure 4a. The top view of the 2D hexagonal lattice corresponding to the *P6/mmm* point group symmetry is shown in Figure 4d. Notably, as shown in Table 2, indexation to the rectangular columnar ($Col_r$) lattice also fits well.

Figure 2b illustrates the 1D intensity versus $2\theta$ profiles obtained for the high (150 °C; red trace) and low (100 °C; blue trace) temperature Col phases of the compound **DLT-10**. The high-temperature (HT) diffraction pattern comprised a set of sharp reflections in the low-angle region besides two diffuse peaks at about 4.6 and 3.4 Å at high angles. The sharp peaks are indexed as the (100), (200), and (3−20) diffractions of a 2D hexagonal lattice with an intercolumnar distance of about 42.2 Å. As can be seen in Figure 2b (blue trace) and Table 2, the low-temperature (LT) Col phase possesses nearly a matching XRD data, of course with some marginal changes in spacing values, to that of the HT columnar ($Col_h$) phase. In fact, low-angle reflections could also be indexed to the $Col_h$ phase, but such an assignment appears unreasonable as both POM and DSC studies clearly indicate the occurrence of two Col phases. However, the possibility of the LT Col phase being another variant of the $Col_h$ phase originating due to the change from planar conformation to propeller geometry of **DLT-10** molecules (within a column) cannot be ruled out. Precise determination of the lattice type is difficult owing to the small number of reflections as the core is very small and there is substantial void in the disc formed by the molecule as indeed seen in Figure 3. The latter, for example, can increase the out-of-plane fluctuations of the discs and thereby prevent a better definition of the lattice. To illustrate this point, the spacings obtained for **DLT-10** in the low as well as high-temperature regions could be indexed to a rectangular lattice (*C*2 *mm* symmetry) with no noticeable change in the error values. As is well-known, the discogens in the rectangular Col phase tilt with respect to the column axis (Figure 4b), and thus, the individual columns appear elliptical when viewed from the top of the 2D


dx.doi.org/10.1021/jo302332u | *J. Org. Chem.* 2013, 78, 527−544

**Table 2. Results of (*hkl*) Indexation of XRD Profiles of the DLT-*n* Series at a Given Temperature (*T*) of Mesophases[a]**

| TSANs (*D*/Å) | phase (T/°C) | $d_{obs}$ (Å) | $d_{cal}$ (Å) | Miller indices *hkl* | lattice parameters (Å), lattice area *S* (Å$^2$), molecular volume *V* (Å$^3$) |
|---|---|---|---|---|---|
| **DLT-8** (46.8) | $Col_{h/r}$ (140) | 34.41 | 34.36 | 100 | *a* = 39.67; *a* = *68.56* |
| | | | (*34.28*) | (*110*), (*200*) | *b* = *39.58* |
| | | 17.13 | 17.18 | 200 | *S* = 1363 *1356.7* |
| | | | (*17.14*) | (*400*),(*220*) | *V* = 4643.5 *4622.2* |
| | | 12.91 | 12.99 | 3−10, 3−20 | (*P6*) (*C2 mm*) |
| | | | (*12.96*) | (*130*), (*420*), (*510*) | *Z* = 1.7 |
| | | 4.60 ($h_a$) | | | |
| | | 3.41 ($h_c$) | | | |
| **DLT-10** (53.9) | $Col_h$ (150) | 36.61 | 36.58 | 100 | *a* = 42.24 *a* = *73.12* |
| | | | (*36.61*) | (*110*), (*200*) | *b* = *42.25* |
| | | 18.27 | 18.29 | 200 | 1545 1547.6 |
| | | | (*18.30*) | (*400*), (*220*) | 5316.2 5324.9 |
| | | 13.76 | 13.83 | 3−10; 3−20 (*130*), (*420*), (*510*) | (*P6*) (*C2 mm*) |
| | | | (*13.84*) | | *Z* = 1.7 *Z* = *1.9* |
| | | 4.66 ($h_a$) | | | |
| | | 3.44 ($h_c$) | | | |
| | $Col_r$ (100) | 37.17 | 37.12 | 100 | *a* = 42.9 *a* = *74.19* |
| | | | (*37.12*) | (*110*), (*200*) | *b* = *42.88* |
| | | 18.53 | 18.56 | 200 | 1591.1 *3181.2* |
| | | | (*18.55*) | (*400*),(*220*) | 5403.5 *10 803.8* |
| | | 13.93 | 14.03 | 3−10, 3−20 | (*P6*) (*C2 mm*) |
| | | | (*14.04*) | (*130*), (*420*), (*510*) | *Z* = 1.8 *Z* = *1.8* |
| | | 4.56 ($h_a$) | | | |
| | | 3.40 ($h_c$) | | | |
| **DLT-12** (55.7) | $Col_h$ (150) | 38.73 | 38.73 | 100 | *a* = 44.7 |
| | | 4.68 ($h_a$) | | | 1731.7 |
| | | 3.46 ($h_c$) | | | 5994.3 |
| | | | | | *Z* = 1.7 |
| | $Col_r$ (60) | 40.02 | *40.02* | *200* | *a* = *80.04*; *b* = *32.06* |
| | | 29.76 | *29.76* | *110* | *1283* |
| | | 19.93 | *20.01* | *400* | *4502.8* |
| | | 4.54 ($h_a$) | | | (*P2 mm*) |
| | | 3.51 ($h_c$) | | | *Z* = *1.4* |

[a]The diameter (*D*) of the disk (estimated from ChemBio3D Ultra 12.0 molecular model software). $d_{obs}$: spacing observed; $d_{cal}$: spacing calculated (deduced from the lattice parameters; *a* for $Col_h$ phase and *a* and *b* for $Col_r$ phase). The spacings marked $h_a$ and $h_c$ correspond to diffuse reflections in the wide-angle region arising from correlations between the alkyl chains and core regions, respectively. *Z* indicates the number of molecules per columnar slice of thickness $h_c$, estimated from the lattice area *S* and the volume *V*. The numbers in italics show the values for the alternate scheme of indexing for rectangular lattice.

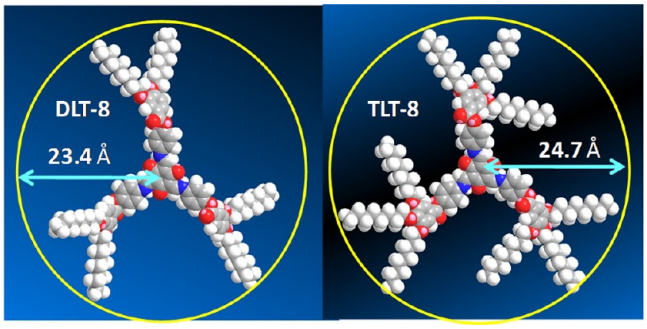


**Figure 3.** Space-filling energy minimized (all-*trans*) molecular models of hekates-TSANs consisting of six (**DLT-8**) and nine (**TLT-8**) peripheral alkoxy tails (derived from the molecular mechanics (MM2) method; see the Supporting Information for XYZ coordinates for these two structures).

lattice structure (see Figure 4e,f). In fact, based on the symmetries assigned to the rectangular 2D lattices, three different $Col_r$ phases, possessing $P2_1/a$ (Figure 4e), $P2/a$, and *C2 mm* (Figure 4f) point group symmetries, have been identified; of these, the mesophase featuring *C2 mm* symmetry is commonly observed in discotic LCs. Table 2 shows the results of such an indexing scheme. However, it should be noted that there is a strong signature of the transition between the two phases in the calorimetric scans. The fact that the transition enthalpy for this columnar−columnar transformation is quite high further supports the possibility of their lattices being of a different type rather than variations of the same variety. In view of this, we suggest that the HT phase is hexagonal and the LT one is rectangular.

As discussed earlier, like the mesogen **DLT-10**, the higher homologue **DLT-12** with six dodecyloxy peripheral tails displays two different columnar phases between the crystalline and the isotropic phase. The X-ray profile of the HT Col phase showed (Figure 2c, red trace) only a strong reflection corresponding to a Bragg spacing *d* of 38.7 Å at the low-angle region, besides two diffuse peaks at about 4.7 and 3.5 Å in the wide angles. The occurrence of only a single maximum at low angles precludes an unequivocal structural assignment; however, as frequently found in the literature,[26,27] such a


dx.doi.org/10.1021/jo302332u | *J. Org. Chem.* 2013, 78, 527−544

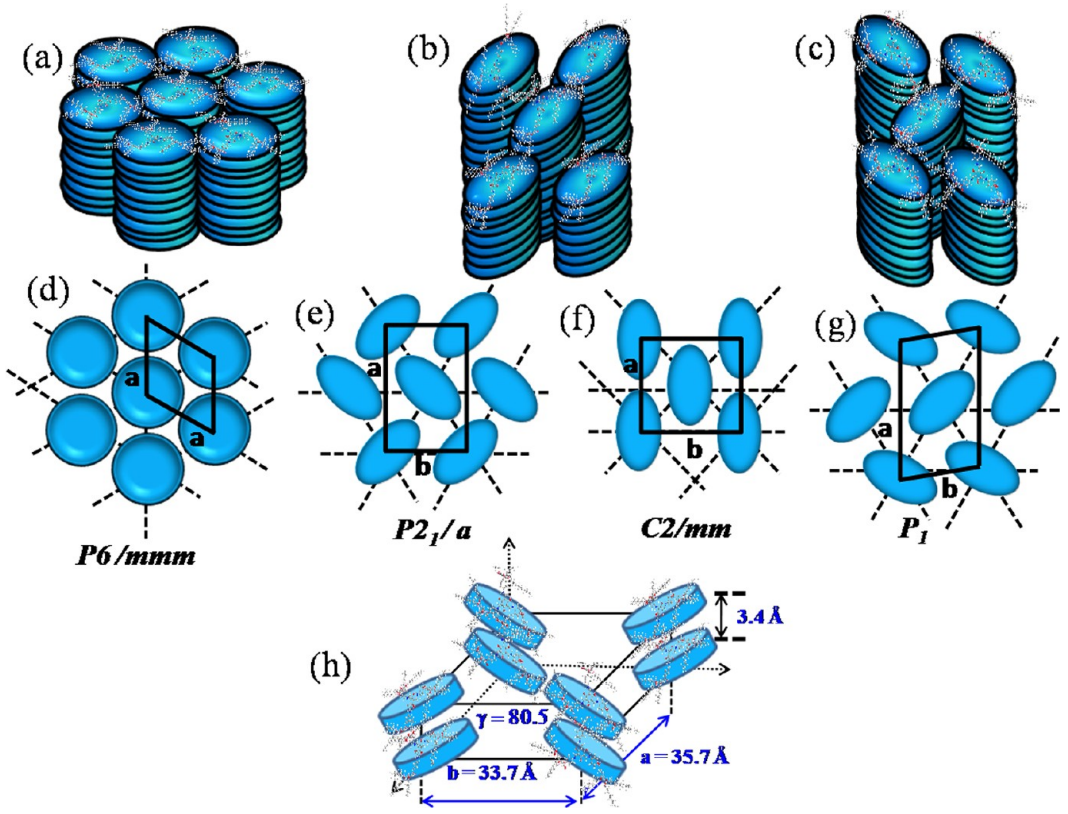


**Figure 4.** Schematic representation (tilted side view) of the self-assembly of hekates-TSANs (shown on top of each column in the form of energy minimized molecular models) in (a) hexagonal columnar, $Col_h$, (b) rectangular columnar, $Col_r$, and (c) oblique columnar, $Col_{ob}$ phases. Top views of the 2D lattices with corresponding point-group symmetries of (d) $Col_h$, (e, f) $Col_r$, and (g) $Col_{ob}$ phases (ellipses indicate the tilting of discogens with respect to columnar axis). A schematic representation of a unit cell of (h) a $Col_{ob}$ phase formed by **TLT-8**; for the sake of clarity, only two molecules are shown in each unit cell.

pattern has been assigned to the Col phase possessing hexagonal symmetry where the absence of other reflections has been ascribed to a minimum in the form factor. The labeling of this HT phase as $Col_h$ would also be in line with the assignment made for the HT phases of the other two **DLT-*n*** compounds. Needless to say, a diffuse halo found at 4.7 Å is typical of the liquidlike order between the aliphatic chains and the adjacent diffuse peak indicating periodic stacking of the discogens within the column at a mean distance of 3.5 Å, a feature characteristic of $\pi$-stacked systems. In essence, for the HT Col phase of **DLT-12**, the XRD study suggests a 2D hexagonal lattice with an intercolumnar distance of about 44.7 Å. For the pattern obtained at 60 °C in the LT mesophase (Figure 2c, blue trace), we consider a rectangular columnar phase following the arguments made above for **DLT-10**. Notably, this phase freezes into a glassy state near room temperature (RT) and remains unaltered until −60 °C (see the DSC trace of cooling cycle shown in Figure 1c). The XRD pattern obtained for this state at RT (25 °C) was found to be analogous to that of the HT (60 °C) pattern confirming the freezing of the 2D structure. This is noteworthy given the fact that such structures facilitate motion of the charges with the concomitant freezing of the ionic impurities.[6b]

Figure 5 depicts the dependence of the onset and clearing temperatures of the **DLT-*n*** series of compounds on the length, number of carbon atoms ($n$) present in the terminal tails. Apparently, the increase in the chain length effectively reduces the melting (onset) temperatures with the increase in the clearing transition temperatures; thus, in this series, the thermal

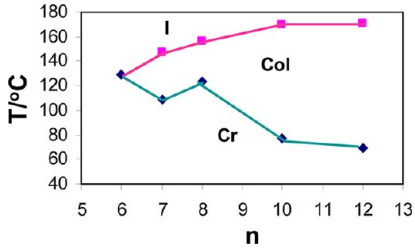


**Figure 5.** Dependence of transition (melting and clearing) temperatures on number of carbon atoms ($n$) in the peripheral alkoxy tails for the **DLT-*n*** series. Note that $Cr_1$−$Cr_2$ and $Col_r$−$Col_h$ transitions are not presented for the sake of clarity. The lines joining points are suggestive of the general trend; note that data do not cover for $n$ = 9 and 11.

range of the Col phase increases with increase in the length of terminal tails.

*Mesomorphic Behavior of the **TLT-n** Series.* The phase sequences, transition temperatures, and associated enthalpies for the **TLT-*n*** series of hekates-TSANs are given in Table 3. These compounds show a different trend in their thermal behavior when compared to the compounds of the **DLT-*n*** series. For example, the lower homologue **TLT-6** with nine *n*-hexyloxy tails of this series, unlike **DLT-6** possessing six *n*-hexyloxy tails of **DLT-n** series, exhibits an enantiotropic Col phase that was evidenced by the observation of an optical texture featuring a combination of mosaics with linear and fan-shaped birefringent defects and homeotropic regions (Figure


dx.doi.org/10.1021/jo302332u | J. Org. Chem. 2013, 78, 527−544

**Table 3. Phase Transition Temperatures[a] (°C) and Corresponding Enthalpies (kJ/mol) of the TLT-*n* Series of Compounds[b]**

| compd TLT-*n* | phase sequence | |
|---|---|---|
| | heating | cooling |
| **TLT-4** | Cr 171.6 [8.5] I | I 154.4 [0.6] $Col_{ob}$[c] 150.5 [3] Cr |
| **TLT-5** | Cr 167.1 [3.1] $Col_{ob}$ 176.7 [2.8] I | I 173.1 [2.8] $Col_{ob}$ 149.5 [2] Cr |
| **TLT-6** | Cr 148.8 [5.6] $Col_{ob}$ 179.2 [3.9] I | I 175.1 [3.9] $Col_{ob}$ 128.6 [0.3] Cr |
| **TLT-7** | Cr 129.8 [1.1] $Col_{ob}$ 168.7 [3.8] I | I 162.7 [3.3] $Col_{ob}$ 122.3[d] Cr |
| **TLT-8** | Cr 129.1 [0.8] $Col_{ob}$ 152.5 [3.5] I | I 147.2 [3.5] $Col_{ob}$ 115.2[d] Cr |
| **TLT-10** | Cr 113.2 [3.8] I | I 100.2 [3.9] Cr |

[a]Peak temperatures in the DSC thermograms obtained during the first heating and cooling cycles at 5 °C/min. [b]$Col_{ob}$: oblique columnar phase. [c]A metastable mesophase. [d]The phase transition was observed under a polarizing microscope and was too weak to be recognized by DSC.

6a). Even the other lower members of this series, namely, **TLT-4** and **TLT-5**, display Col behavior with a similar texture, as shown in Figure 6b; however, in the former case, the mesophase was found to be metastable. This suggests that these compounds facilitate the optimal space filling. The higher homologues, namely, discogens **TLT-7** and **TLT-8**, display an enantiotropic Col phase exhibiting optical textures that are similar to those observed for **TLT-4**, **TLT-5**, and **TLT-6**. It may be remarked here that, for both the compounds **TLT-7** and **TLT-8**, the signature due to the Col−Cr transition in the DSC traces of cooling cycles could not be detected, although this phase transition was clearly seen by POM; the DSC traces of **TLT-8** shown in Figure 6b illustrate the same. Thus, the findings of the optical textural study clearly suggest that all the discogens of the **TLT-*n*** series, with the exception of **TLT-10**, exhibit an analogous columnar mesomorphism. Surprisingly, the discogen **TLT-10** did not show mesomorphism, unlike its analogous compound **DLT-10** with six *n*-decyloxy tails belonging to the **DLT-*n*** series. However, this hekates shows a much lower clearing (Cr−I) temperature than other members of the series. Therefore, it can be contemplated that the disc broadening (due to the presence of longer alkoxy tails) weakens the side-on (face-to-face) interaction that results in the lower clearing points with the suppression of mesomorphism and thus renders the compound nonmesomorphic. In other words, owing to strong core−core (face-to-face) correlation, which results from the constrained packing of cores possessing short or medium alkoxy tail lengths, leads to columnar behavior. Thus, in this **TLT-*n*** series, as illustrated in Figure 7, on

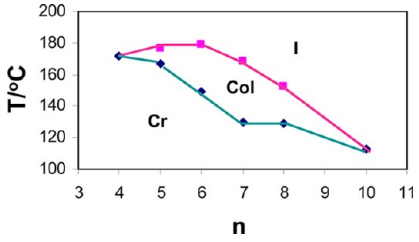


**Figure 7.** Dependence of the transition (melting and clearing) temperatures on the carbon atoms ($n$) in the peripheral alkoxy tails for the **TLT-*n*** series. The lines joining points are suggestive of the general trend; it may be noted that experimental data do not cover for $n$ = 9.

increasing the lengths of peripheral alkoxy tails, strong reduction in the clearing temperature occurs that leads to the suppression of the mesophase unlike in the **DLT-*n*** series (see Figure 5).

It may be reiterated here that all the discogens of this series, except **TLT-10**, irrespective of the variation in the length of nine peripheral tails, stabilize an identical Col phase that was ascertained substantially based on the optical textural pattern. In fact, in the miscibility study, by means of contact preparation, the Col phase of all the discogens could be well mixed with the mesophases formed by **TLT-6** and **TLT-8**. Thus, the structures of mesophases of these two discotics, as representative cases, were characterized with the aid of XRD technique. Figure 8a,b shows the X-ray diagrams of the Col

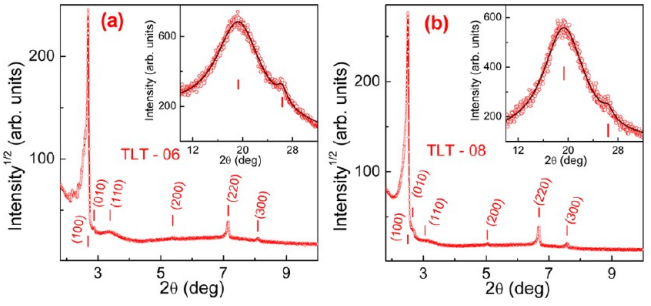


**Figure 8.** 1D XRD profiles plotting the diffraction intensity against the $2\theta$ obtained for the Col phase of compounds (a) **TLT-6** and (b) **TLT-8**.

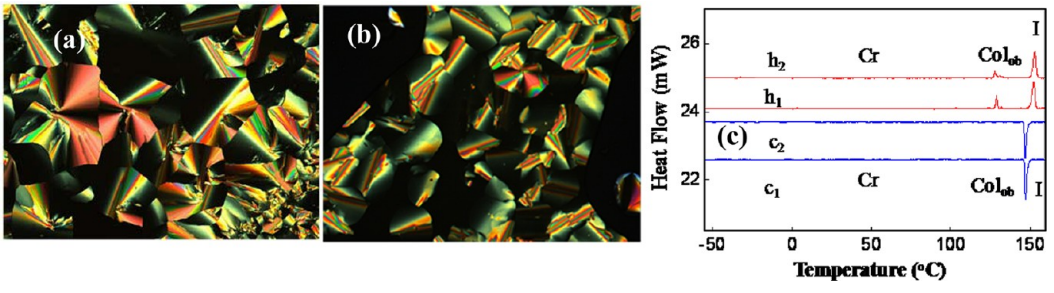


**Figure 6.** (a) Photomicrograph of optical texture obtained for the $Col_{ob}$ phase of **TLT-6** at 170 °C. (b) Microphotograph of textural pattern seen for the $Col_{ob}$ phase of **TLT-4** at 153 °C. (c) DSC traces obtained during the first and second heating ($h_1$ and $h_2$) and cooling ($c_1$ and $c_2$) cycles of compound **TLT-8**.


dx.doi.org/10.1021/jo302332u | J. Org. Chem. 2013, 78, 527−544

phases of **TLT-6** and **TLT-8**, respectively, which appear nearly identical. The indexed diffractions of 1D intensity versus $2\theta$ profile of the mesophases and the results emanating from these studies are summarized in Table 4. As can be seen, the

**Table 4. Results of Indexation of XRD Profiles of the TLT-*n* Series at a Given Temperature ($T$) of Col Phases[a]**

| TSANs ($D$/Å) | phase ($T$/°C) | $d_{obs}$ (Å) | $d_{cal}$ (Å) | Miller indices $hkl$ | lattice parameters (Å), lattice area $S$ (Å$^2$), molecular volume $V$ (Å$^3$) |
|---|---|---|---|---|---|
| **TLT-6** (42.9) | $Col_{ob}$ (160) | 32.91 | 32.88 | 100 | $a$ = 33.4; $b$ = 31.25; $\gamma$ = 79.9° |
| | | 30.77 | 30.77 | 010 | $S$ = 1027.5 |
| | | 26.13 | 24.73 | 110 | $V$ = 3476.1 |
| | | 16.41 | 16.44 | 200 | $Z$ = 1.12 |
| | | 12.36 | 12.36 | 220 | |
| | | 10.92 | 10.96 | 300 | |
| | | 4.59 ($h_a$) | | – | |
| | | 3.38 ($h_c$) | | | |
| **TLT-8** (49.4) | $Col_{ob}$ (140) | 35.20 | 35.16 | 100 | $a$ = 35.65; $b$ = 33.74; $\gamma$ = 80.5° |
| | | 33.27 | 33.27 | 010 | 1186.3 |
| | | 28.93 | 26.45 | 110 | 4001.7 |
| | | 17.53 | 17.58 | 200 | $Z$ = 1.14 |
| | | 13.23 | 13.23 | 220 | |
| | | 11.67 | 11.72 | 300 | |
| | | 4.59 ($h_a$) | | – | |
| | | 3.37 ($h_c$) | | | |

[a] $Col_{ob}$: oblique columnar phase. The diameter ($D$) of the disk (estimated from ChemBio3D Ultra 12.0 molecular model software). $d_{obs}$: spacing observed; $d_{cal}$: spacing calculated (deduced from the lattice parameters $a$ and $b$ and column tilt angle $\gamma$. The spacings marked $h_a$ and $h_c$ correspond to diffuse reflections in the wide-angle region arising from correlations between the alkyl chains and core regions, respectively (solid line in the inset is a fit to a Lorentzian expression). $Z$ indicates the number of molecules per columnar slice of thickness $h_c$, estimated from the lattice area $S$ and the volume $V$.

diffractograms of **TLT-6** and **TLT-8** show two broad, diffuse scattering halo in the wide-angle region (see Figure 8 and Table 4) arising due to the liquidlike order of the aliphatic chains and correlation between molecular cores of discogens within the same column. In the low-angle regions, several sharp reflections along with a very weak reflection were observed for both the discogens with the spacing being 32.91, 30.77, 26.13, 16.41, 12.36, and 10.92 Å for **TLT-6** and 35.20, 33.27, 28.93, 17.53, 13.23, and 11.67 Å for **TLT-8**, which were respectively assigned as the (100), (010), (110), (200), (220), and (300) diffractions. As shown in Table 4, these two sets of reflections could be indexed to 2D oblique lattices; hence, we assign the phases to be an oblique columnar phase ($Col_{ob}$) with the following unit cell parameters: $a$ = 33.40 Å, $b$ = 31.25 Å, and column tilt angle $\gamma$ = 79.9° for **TLT-6**; and $a$ = 35.65 Å, $b$ = 33.74 Å, and $\gamma$ = 80.5° for **TLT-8** (see Figure 4h). However, it may be noted here that these two lattices are nearly close to a rectangular cell as the angle ($\gamma$) between the lattice parameters, $a$ and $b$, are very close to 90°. The symmetry of the 2D lattice can be identified as $P_1$, which being a primitive class space group, as it allows all diffractions. Each column of the $Col_{ob}$ phase, when viewed from the top, appears elliptical (Figure 4c) where the constituent discogens in the columns tilt by an angle ($a$) with respect to the columnar axis that is perpendicular to the normal of the lattice plane (Figure 4g). The occurrence of the $Col_{ob}$ phase in these compounds is noteworthy in view of the fact that such a phase occurs less commonly and in fact it originates as a consequence of the intense core−core correlations.[4,19,28] Thus, hekates-TSANs surrounded by nine alkoxy flexible chains, unlike their six alkoxy-substituted counterparts, pack very intensively to form columns. It is also important to note that analogous hekates-TSANs appended with 1,3,4-oxadiazole fluorophores display a columnar phase featuring hexagonal symmetry.[9d] Furthermore, the short-armed TSANs with a similar number of peripheral alkoxy chains stabilize hexagonal and rectangular Col phases in a dimesomorphic sequence (see Chart 2 for molecular structures).[9c] Hence, the **TLT-*n*** series represents the first examples of discotic TSANs exhibiting a scarcely reported $Col_{ob}$ phase. Presently, we are unable to provide a logical reasoning or provide an appropriate explanation for such a behavior.

**Photophysical Properties.** In recent years, it is well demonstrated that TSANs are a unique class of organic systems where the luminescence and molecular material features such as self-organizing ability, molecular recognition, and so forth can be imbued readily.[9−11] Over the years, our group has especially illustrated that by rational molecular design, functional TSANs can be accomplished exhibiting self-assembling ability into the Col phase as well as light emission, which are promising features for emissive LC displays[29] and organic light-emitting devices (OLEDs).[30] Most importantly, we have realized that the fluorescence behavior can be tuned by varying the chemical (electronic) nature of the three substituents (arms) around the central cyclohexane-1,3,5-trione core. The present hekates-TSANs have been prepared to understand the effect on photophysical properties when semiflexible benzoate long arms are attached to the central core. Thus, UV−vis absorption and fluorescence characteristics of one of the representative compounds randomly selected from each series of long-armed TSANs, namely, **DLT-12**, and **TLT-8**, were studied for their solution and mesophase/glassy states. The blue and orange traces in the upper panels of Figure 9a,b are the solution (in THF) absorption and fluorescence spectra of the compounds **DLT-12** and **TLT-8**, respectively.

The absorption spectra obtained for the solutions of **DLT-12** and **TLT-8** show two absorption maxima centered around 325 and 401 nm due to $\pi-\pi^*$ and $n-\pi^*$ transitions, respectively (Table 5). Thus, these absorption maxima show a noticeable hypsochromic (blue) shift when compared to those obtained for short-armed TSANs.[9c] For both the compounds, a fluorescence band at 455 nm was observed with a negligible shoulder when their solutions were irradiated with 400 nm absorption maximum. In fact, as can be seen in the insets of Figure 9, blue light is visually perceivable in the emissive state; it may be pointed out here that green light was observed for short-armed TSANs.[9c] The Stokes shift, which is the difference between the spectral positions of the band maxima of the absorption and emission originating from the same electronic transition, was found to be 54 nm as shown in Table 5; this redshift in the emission band is in agreement with the general experimental observation.[31]

The absorption and fluorescence spectra were also recorded for the thin films of both compounds. The requisite thin films were prepared by keeping these samples between the two coverslips and cooling slowly (1 °C/min) from the isotropic liquid state to RT. To begin with, the absorption spectra were


dx.doi.org/10.1021/jo302332u | J. Org. Chem. 2013, 78, 527−544

**Chart 2. Molecular Structures of (A) 1,3,4-Oxadiazole-based Hekates-TSANs Comprising Nine Peripheral Alkoxy Tails and (B) Short-Armed TSANs with Nine Alkoxy Chains Pertaining to the Previous Studies**

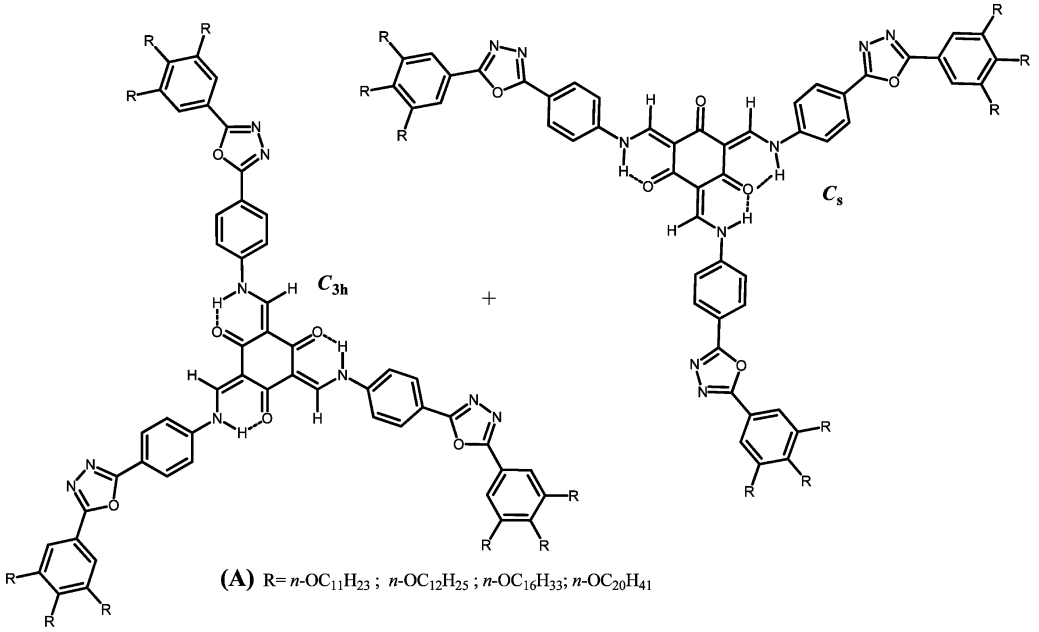


**(A)** R= *n*-$OC_{11}H_{23}$ ; *n*-$OC_{12}H_{25}$ ; *n*-$OC_{16}H_{33}$; *n*-$OC_{20}H_{41}$

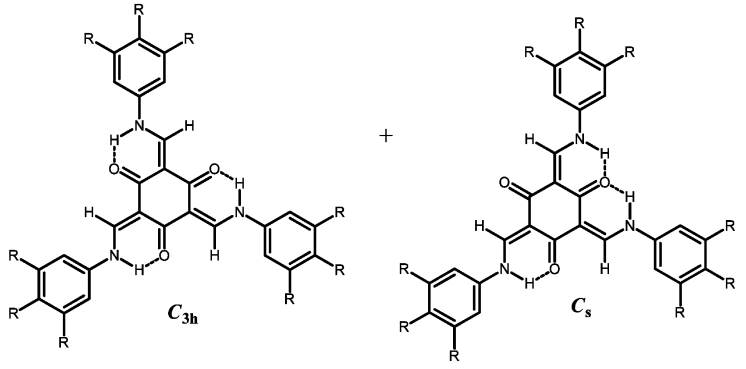


**(B)** R = *n*-$OC_nH_{2n+1}$ and 3,7-Dimethyloctyloxy

recorded at RT where the Col structure freezes in a glassy state. As expected, two absorption bands appear with equal intensity, as shown in the lower left-hand side (LHS) panels of Figure 9a,b; a marginal blueshift (~11−16 nm) can be seen for the absorption bands of both the transitions when compared to the short-armed TSANs reported earlier.[9c] As shown in the lower right-hand side (RHS) panels of Figure 9a,b, these glassy films on exciting at 400 nm show two broad emission bands with a large Stokes shift of around 187−189 nm. This large redshift can be attributed to the intimate overlap of the cores in the glassy film state that brings the energy levels closer. The broad emission band and broadening of absorption and emission bands with redshift are known to be originating from the *J*-type aggregates.[32] On recording the fluorescence spectra as a function of temperature from this glassy state, the pattern of the emissive spectra remains the same, while their intensity reduces progressively and even remains in the isotropic phase. The decrease in fluorescence intensity can be ascribed to thermally activated radiationless processes[33] or breaking of larger columnar stacks. But, this problem could be circumvented as these compounds could be annealed in the glassy state by freezing them in the mesophase. Thus, the frozen Col phase of these compounds could serve as an ideal candidate for the application in OLEDs. The observed redshift in the film state can also be attributed to the formation of excimers or aggregates.[34] More sophisticated techniques such as the effect of annealing on film properties, microscopy to examine film morphology, studies concerning solvent effect on emission and absorption, lifetime studies, and electrochemical studies are required to further elucidate the precise mechanism for the redshift observed in these specific materials.

## ■ SUMMARY

In continuation of our ongoing studies, we have rationally designed and synthesized two (**DLT-*n*** and **TLT-*n***) series of novel star-shaped (hekates) TSANs where three extended (long) arms, in the form of phenyl benzoate substituted with six/nine peripheral *n*-alkoxy tails, have been covalently linked to a central shape-persistent, self-complementing core. This work has been carried out to further our understanding of the effect of chemical (electronic) nature of three arms on the mesomorphic and photophysical properties of what could be a vast family of discotic TSANs. Hekates-TSANs of both the series, with the exception of a few, exhibit Col mesomorphism. In the first (**DLT-*n***) series, the clearing temperature and thus the thermal range of the Col phase increases when the length of six peripheral *n*-alkoxy tails is increased. On the other hand, in the second (**TLT-*n***) series of TSANs, on increasing the lengths


dx.doi.org/10.1021/jo302332u | *J. Org. Chem.* 2013, 78, 527−544

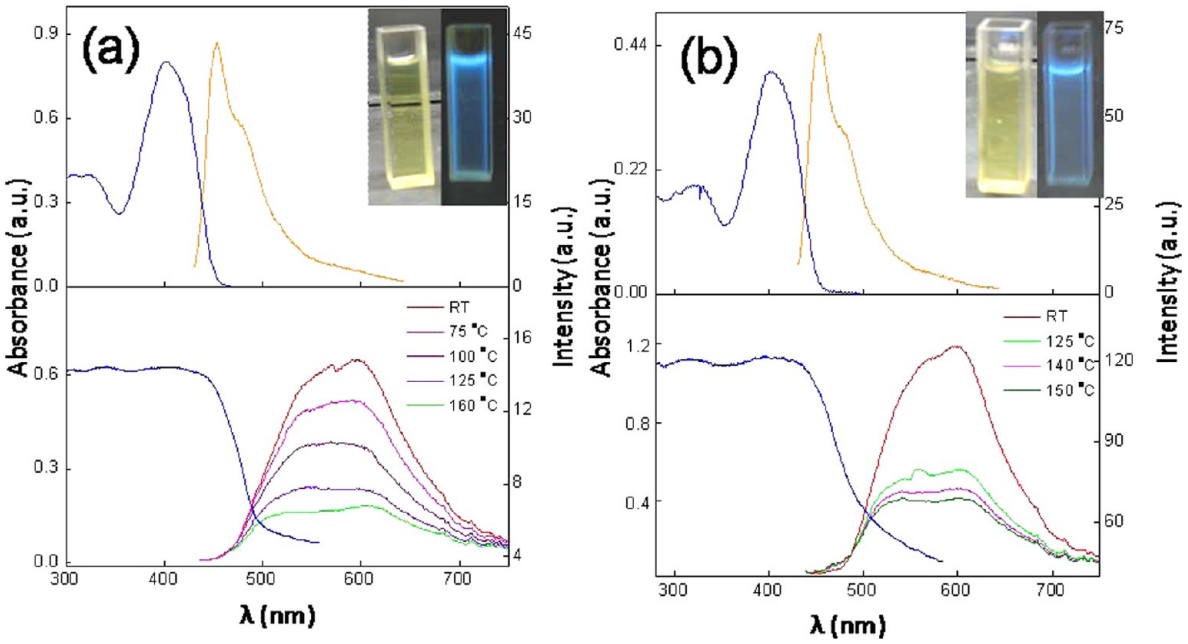


**Figure 9.** Absorption and emission spectra in THF solution (top panels) and in the thin films of the mesophases (lower panels) obtained for (a) **DLT-12** and (b) **TLT-8**; inset shows the pictures of solutions as seen without (LHS) and with the illumination (RHS) of 365 nm light. Note that, for thin films of the Col phase, the spectra were recorded as a function of temperature (see RHS traces of lower panels). (LHS = left-hand side; RHS = right-hand side.)

**Table 5. Photophysical Properties of Hekates-TSANs**

| | THF solution[a] | | | glassy film | | |
|---|---|---|---|---|---|---|
| compd | absorption[b] | emission[bc] | Stokes shift[b] | absorption[b] | emission[bc] | Stokes shift[b] |
| **DLT-12** | 325, 401 | 455 | 54 (2960 $cm^{-1}$) | 342, 408 | 536, 597 | 189 (7759 $cm^{-1}$) |
| **TLT-8** | 323, 401 | 455 | 54 (2960 $cm^{-1}$) | 316, 407 | 540, 594 | 187 (7735 $cm^{-1}$) |

[a]Micromolar solutions in THF. [b]Wavelengths (nm). [c]The excitation wavelength $\lambda_{ex}$ = 400 nm.

of nine peripheral alkoxy tails, a strong reduction in clearing temperature occurs with the suppression of the Col phase thermal width. XRD technique coupled with textural study evidenced the hexagonal and rectangular symmetry of the Col phases formed by the **DLT-*n*** of compounds, while **TLT-*n*** series of discogens with nine flexible tails stabilize the oblique columnar phase and thus are first of their kind. These observations clearly indicate the critical dependence of columnar mesomorphic behavior of these compounds on the number and length of peripheral tails they possess. However, such molecular structural effects are not seen in their light absorption and emission behavior; the representative hekates-TSANs chosen from each series display identical photophysical properties in both solution and mesophase states. The blue light emission observed in the solution state is especially noteworthy. The presence of the ester group and hence the possible transformation from planar to propeller conformation of the wings would have contributed to their overall different behavior when compared to short-armed TSANs reported earlier by our group.

## EXPERIMENTAL SECTION

**General.** All chemicals, namely, gallic acid, 4-nitrophenol, 3,4-dihydroxybenzaldehyde, *n*-bromoalkanes, *N*,*N*′-dicyclohexylcarbodiimide (DCC), 4-dimethylaminopyridine (DMAP), and 10% Pd−C, were used as received from commercial sources without further purification. DMF was allowed to stand for 10 h on KOH pellets before being distilled under reduced pressure; it was then stored over molecular sieves (4 Å) for about two days before use. THF was distilled from sodium and benzophenone under inert atmosphere. Acetone was stored over anhydrous potassium carbonate prior to being distilled. High purity, dry nitrogen was generally used to maintain inert atmosphere conditions. Silica gel (60−120, 100−200, and 230−400 mesh) and neutral aluminiun oxide were used as the stationary phase for column chromatographic purifications. Aluminum sheets precoated with silica gel were employed for thin-layer chromatography, and IR spectra were recorded on a Fourier transform IR spectrometer; the spectral positions are given in wavenumber ($cm^{-1}$) units. $^1H$ (200 and 400 MHz) and $^{13}C$ (100 MHz) NMR spectra were recorded at RT using $CDCl_3$. The chemical shifts are reported in parts per million relative to TMS as an internal standard. Coupling constants are expressed in hertz. In order to illustrate the coupling between the enamine and the NH protons, $^1H-^1H$ COSY NMR spectra were recorded. Mass spectra were measured with a $FAB^+$-MS mass spectrometer using 3-nitrobenzyl alcohol as a liquid matrix. Electronic absorption (UV−vis) and emission spectra of the solution and mesomorphic states were recorded by employing commercial instruments. Photoluminescence spectra of the fluid columnar phase were recorded as a function of temperature with the help of a spectrofluorimeter. Solvents for spectroscopy were spectroscopic grade and were used as received, without any purification.

Thermal behavior and LC property of the mesogenic TSANs were studied by hot-stage polarizing microscopy using a microscope equipped with a temperature-controlled hot-stage. Clean glass slides were used to examine the LC (the birefringence and fluidity) property of the samples. The transition temperatures and associated enthalpies were determined by DSC under nitrogen atmosphere. Peak temperatures in the DSC traces due to phase transitions of the samples were


dx.doi.org/10.1021/jo302332u | J. Org. Chem. 2013, 78, 527−544

found to be in agreement with those of the optical experiments. The transition temperatures obtained from calorimetric measurements of the first heating and cooling cycles at a rate of 5 °C/min are presented; in the cases where the signatures are not observed in the DSC traces, the transition temperatures have been taken from microscopic observations. XRD measurements were carried out on powder (unaligned) samples. The samples were filled in a Lindemann capillary (1 mm diameter) tube in the isotropic phase, and both ends of the tube were flame sealed. The experiments were carried out using Cu K$\alpha$ radiation ($\lambda$ = 1.5418 Å) using a commercial X-ray diffractometer consisting of a focusing elliptical mirror and a fast resolution detector.

**Synthesis.** The synthetic procedures and characterization data for the known precursors **1a**–**e**,[23] **2a**–**e**,[23b] **5**, **6a**–**f**,[24] and **7a**–**f**[25], unknown intermediates **3a**–**e**, **4a**–**e**, **8a**–**f**, and **9a**–**f**, and the target **DLT-*n*** and **TLT-*n*** series of discotics **9a**–**f** are given below.

*General Procedure for the Synthesis of 3,4-Bis(n-alkoxy)-benzaldehydes (**1a**–**e**).* A mixture of 3,4-dihydroxybenzaldehyde (0.25 g, 1.81 mmol, 1 equiv), anhyd $K_2CO_3$ (1.2 g, 8.7 mmol, 4.8 equiv), and the appropriate *n*-bromoalkane (4 mmol, 2.2 equiv) were taken in dry DMF (20 mL) and heated at 80 °C for 12 h under nitrogen atmosphere. The reaction mixture was poured into ice–water and extracted with dichloromethane. The combined extracts were washed with water and brine, dried over anhyd $Na_2SO_4$, and concentrated. The crude product was purified by column chromatography on neutral alumina. Elution with hexanes followed by 5–10% EtOAc–hexanes yielded the desired product. Yields of these compounds were in the range 78–84%.

*3,4-Bis(hexyloxy)benzaldehyde (**1a**).* $R_f$ = 0.50 (10% EtOAc–hexanes); viscous liquid,[23] yield: 0.43 g, (78%). IR (KBr pellet): $\nu_{max}$ in $cm^{-1}$ 2923, 2850, 1686, 1673, 1585, 1510, 1467, 1439, 1391, 1279, 1238, 1166, 1134, 1014, 865, 808, 723, 659, 587. $^1$H NMR ($CDCl_3$, 200 MHz): $\delta$ 9.83 (s, 1H, CHO), 7.41–7.44 (m, 2H, Ar), 6.95 (d, 1H, $J$ = 8 Hz), 4.07 (q, 4H, $J$ = 6.4 Hz, 2 × $OCH_2$), 0.87–1.9 (m, 22H, 8 × $CH_2$, 2 × $CH_3$). MS (FAB+): $m/z$ for $C_{19}H_{31}O_3$ [M + 1], Calcd: 307.2. Found: 307.2. Anal. Calcd for $C_{19}H_{30}O_3$: C, 74.47; H, 9.87. Found: C, 74.6; H, 9.7.

*3,4-Bis(heptyloxy)benzaldehyde (**1b**).* $R_f$ = 0.51 (10% EtOAc–hexanes); white solid, mp: 48–49 °C (lit.[23] mp: 47–49 °C); yield: 0.48 g (80%). IR (KBr pellet): $\nu_{max}$ in $cm^{-1}$ 2924, 2852, 1684, 1671, 1586, 1509, 1466, 1436, 1390, 1280, 1239, 1167, 1134, 1013, 866, 807, 724, 655, 584. $^1$H NMR ($CDCl_3$, 200 MHz): $\delta$ 9.83 (s, 1H, CHO), 7.40–7.44 (m, 2H, Ar), 6.95 (d, 1H, $J$ = 8 Hz), 4.07 (q, 4H, $J$ = 6.6 Hz, 2 × $OCH_2$), 0.86–1.9 (m, 26H, 10 × $CH_2$, 2 × $CH_3$). MS (FAB+): $m/z$ for $C_{21}H_{34}O_3$, Calcd: 334.25. Found: 334.1. Anal. Calcd for $C_{21}H_{34}O_3$: C, 75.41; H, 10.25. Found: C, 75.6; H, 10.1.

*3,4-Bis(octyloxy)benzaldehyde (**1c**).* $R_f$ = 0.48 (10% EtOAc–hexanes); white solid, mp: 53–55 °C (lit.[23] mp: 52–54 °C); yield: 0.54 g, (83%). IR (KBr pellet): $\nu_{max}$ in $cm^{-1}$ 2924, 2850, 1683, 1673, 1584, 1511, 1466, 1434, 1391, 1283, 1240, 1164, 1132, 1511, 1012, 865, 811, 722, 654, 583. $^1$H NMR ($CDCl_3$, 200 MHz): $\delta$ 9.83 (s, 1H, CHO), 7.40–7.43 (m, 2H, Ar), 6.95 (d, 1H, $J$ = 8 Hz), 4.07 (q, 4H, $J$ = 6.4 Hz, 2 × $OCH_2$), 0.85–1.9 (m, 30H, 12 × $CH_2$, 2 × $CH_3$). MS (FAB+): $m/z$ for $C_{23}H_{38}O_3$, Calcd: 362.28. Found: 362.1. Anal. Calcd for $C_{23}H_{38}O_3$: C, 76.2; H, 10.56. Found: C, 76.3; H, 10.7.

*3,4-Bis(decyloxy)benzaldehyde (**1d**).* $R_f$ = 0.48 (10% EtOAc–hexanes); white solid, mp: 65–66 °C (lit.[23] mp: 65 °C); yield: 0.64 g (84%). IR (KBr pellet): $\nu_{max}$ in $cm^{-1}$ 2922, 2850, 2345, 1683, 1672, 1586, 1509, 1467, 1440, 1393, 1278, 1236, 1134, 1511, 1012, 865, 808, 659. $^1$H NMR ($CDCl_3$, 200 MHz): $\delta$ 9.83 (s, 1H, CHO), 7.39–7.44 (m, 2H, Ar), 6.95 (d, 1H, $J$ = 8 Hz), 4.02–4.11 (q, 4H, $J$ = 6.4 Hz, 2 × $OCH_2$), 0.85–1.9 (m, 38H, 16 × $CH_2$, 2 × $CH_3$); MS (FAB+): $m/z$ for $C_{27}H_{47}O_3$ [M + 1], Calcd: 419.3. Found: 419.5. Anal. Calcd for $C_{27}H_{46}O_3$: C, 77.46; H, 11.07. Found: C, 77.3; H, 11.2.

*3,4-Bis(dodecyloxy)benzaldehyde (**1e**).* $R_f$ = 0.49 (10% EtOAc–hexanes); white solid, mp: 71–72 °C (lit.[23] mp: 71 °C); yield: 0.71 g, (82%); IR (KBr pellet): $\nu_{max}$ in $cm^{-1}$ 2919, 2850, 1683, 1671, 1586, 1509, 1467, 1440, 1393, 1278, 1236, 1134, 1069, 1012, 808, 659. $^1$H NMR ($CDCl_3$, 200 MHz): $\delta$ 9.83 (s, 1H, CHO), 7.39–7.44 (m, 2H, Ar), 6.95 (d, 1H, $J$ = 8 Hz), 4.02–4.11 (q, 4H, $J$ = 6.4 Hz, 2 × $OCH_2$), 0.85–1.9 (m, 46H, 20 × $CH_2$, 2 × $CH_3$). MS (FAB+): $m/z$ for $C_{31}H_{54}O_3$, Calcd: 474.41. Found: 474.3. Anal. Calcd for $C_{31}H_{54}O_3$: C, 78.43; H, 11.46. Found: C, 78.6; H, 11.3.

*General Procedure for the Synthesis of 3,4-Bis(alkoxy)benzoic acids (**2a**–**e**).* To a solution of 3,4-bis(alkoxy)benzaldehyde (**1a**–**e**) (7.2 mmol, 1 equiv) in acetone (30 mL) was added freshly prepared Jones reagent (5 equiv) dropwise to get an orange solution. The reaction mixture was stirred for an hour. Addition of water leads to the formation of thick precipitate of acid, which was filtered and washed with water. The solid was dissolved in dichloromethane and washed with water and brine, dried over anhyd $Na_2SO_4$, and concentrated. The crude product was recrystallized with hexanes. In the case of higher homologues, boiling the solid with hot hexanes followed by filtration removed the unreacted starting material. Yields of these compounds were in the range 80–86%.

*3,4-Bis(hexyloxy)benzoic Acid (**2a**).* $R_f$ = 0.3 (50% EtOAc–hexanes); white solid, mp: 128–130 °C (lit.[23b] mp: 128 °C); yield: 2.0 g (86%). IR (KBr pellet): $\nu_{max}$ in $cm^{-1}$ 2926, 2850, 1670, 1596, 1467, 1442, 1308, 1278, 1227, 1140, 1069, 941, 870, 647. $^1$H NMR ($CDCl_3$, 200 MHz): $\delta$ 7.72 (dd, 1H, $J$ = 2 Hz, 8.4 Hz, Ar), 7.58 (d, 1H, $J$ = 1.6 Hz, Ar), 6.89 (d, 1H, $J$ = 8.6 Hz), 4.02–4.1 (m, 4H, 2 × $OCH_2$), 0.86–1.88 (m, 22H, 8 × $CH_2$, 2 × $CH_3$). MS (FAB+): $m/z$ for $C_{19}H_{31}O_4$ [M + 1], Calcd: 323.21. Found: 323.2. Anal. Calcd. for $C_{19}H_{30}O_4$: C, 70.77; H, 9.38. Found: C, 70.71; H, 9.5.

*3,4-Bis(heptyloxy)benzoic Acid (**2b**).* $R_f$ = 0.30 (50% EtOAc–hexanes); white solid, mp: 125–127 °C (lit.[23b] mp: 127 °C); yield: 2.1 g (83%). IR (KBr pellet): $\nu_{max}$ in $cm^{-1}$ 2924, 2849, 1671, 1598, 1466, 1441, 1309, 1276, 1226, 1139, 1070, 942, 871, 645. $^1$H NMR ($CDCl_3$, 200 MHz): $\delta$ 7.72 (dd, 1H, $J$ = 2 Hz, 8.4 Hz, Ar), 7.59 (d, 1H, $J$ = 1.6 Hz, Ar), 6.89 (d, 1H, $J$ = 8.6 Hz), 4.02–4.1 (m, 4H, 2 × $OCH_2$), 0.86–1.88 (m, 26H, 10 × $CH_2$, 2 × $CH_3$); MS (FAB+): $m/z$ for $C_{21}H_{34}O_4$, Calcd: 350.25. Found: 350.2. Anal. Calcd for $C_{21}H_{34}O_4$: C, 71.96; H, 9.78. Found: C, 72.1; H, 9.64.

*3,4-Bis(octyloxy)benzoic Acid (**2c**).* $R_f$ = 0.30 (50% EtOAc–hexanes); white solid, mp: 123–124 °C (lit.[23b] mp: 125 °C); yield: 2.2 g (80%); IR (KBr pellet): $\nu_{max}$ in $cm^{-1}$ 2928, 2845, 1670, 1598, 1467, 1442, 1308, 1278, 1227, 1140, 1070, 941, 870, 647. $^1$H NMR ($CDCl_3$, 200 MHz): $\delta$ 7.74 (dd, 1H, $J$ = 1.6 Hz, 8.4 Hz, Ar), 7.58 (d, 1H, $J$ = 1.6 Hz, Ar), 6.89 (d, 1H, $J$ = 8.6 Hz), 4.02–4.1 (m, 4H, 2 × $OCH_2$), 0.86–1.88 (m, 30H, 12 × $CH_2$, 2 × $CH_3$). MS (FAB+): $m/z$ for $C_{23}H_{38}O_4$, Calcd: 378.3. Found: 378.5. Anal. Calcd for $C_{23}H_{38}O_4$: C, 72.98; H, 10.12. Found: C, 72.67; H, 9.91.

*3,4-Bis(decyloxy)benzoic Acid (**2d**).* $R_f$ = 0.30 (50% EtOAc–hexanes); white solid, mp: 121–122 °C (lit.[23b] mp: 123 °C); yield: 2.6 g (82%). IR (KBr pellet): $\nu_{max}$ in $cm^{-1}$ 2924, 2842, 1676, 1598, 1466, 1442, 1308, 1278, 1227, 1141, 1070, 769. $^1$H NMR ($CDCl_3$, 200 MHz): $\delta$ 7.73 (dd, 1H, $J$ = 1.6 Hz, 8.4 Hz, Ar), 7.58 (d, 1H, $J$ = 1.6 Hz, Ar), 6.89 (d, 1H, $J$ = 8.6 Hz), 4.02–4.1 (m, 4H, 2 × $OCH_2$), 0.86–1.88 (m, 38H, 16 × $CH_2$, 2 × $CH_3$). MS (FAB+): $m/z$ for $C_{27}H_{46}O_4$, Calcd: 434.34. Found: 434.6. Anal. Calcd for $C_{27}H_{46}O_4$: C, 74.61; H, 10.67. Found: C, 74.8; H, 10.8.

*3,4-Bis(dodecyloxy)benzoic Acid (**2e**).* $R_f$ = 0.30 (50% EtOAc–hexanes); white solid, mp: 119–121 °C (lit.[23b] mp: 121 °C); yield: 2.94 g (84%). IR (KBr pellet): $\nu_{max}$ in $cm^{-1}$ 2919, 2850, 1674, 1596, 1466, 1443, 1307, 1277, 1227, 1141, 1070, 769. $^1$H NMR ($CDCl_3$, 200 MHz): $\delta$ 7.72 (dd, 1H, $J$ = 2 Hz, 8.4 Hz, Ar), 7.62 (d, 1H, $J$ = 1.6 Hz, Ar), 6.93 (d, 1H, $J$ = 8.6 Hz), 4.06–4.14 (m, 4H, 2 × $OCH_2$), 0.89–1.89 (m, 46H, 20 × $CH_2$, 2 × $CH_3$). MS (FAB+): $m/z$ for $C_{31}H_{54}O_4$, Calcd: 490.4. Found: 490.3. Anal. Calcd for $C_{31}H_{54}O_4$: C, 75.87; H, 11.09. Found: C, 75.9; H, 11.2.

*General Procedure for the Synthesis of 4-Nitrophenyl 3,4-Dialkoxybenzoates (**3a**–**e**).* A mixture of 3,4-bis(*n*-alkoxy)benzoic acid (**2a**–**e**) (2.3 mmol, 1 equiv) and 4-nitrophenol (0.32 g, 2.3 mmol, 1 equiv) were dissolved in dry THF (20 mL), degassed, and stirred under nitrogen atmosphere. To this solution, was added a solution of DCC (0.712 g, 3.45 mmol, 1.5 equiv) and a catalytic amount of DMAP (0.015 g, 0.12 mmol, 0.05 equiv) in THF (10 mL). The reaction mixture was stirred at RT for 12 h under inert (nitrogen) atmosphere. The precipitated dicyclohexylurea was filtered off, and the combined filtrate was concentrated. The residue was dissolved in ethyl acetate, washed with 5% cold NaOH(aq) solution, water, and brine,


dx.doi.org/10.1021/jo302332u | J. Org. Chem. 2013, 78, 527–544

dried over anhyd $Na_2SO_4$, and concentrated. The crude product was purified by column chromatography using silica gel (100−200). Elution with hexanes followed by 5% EtOAc−hexanes yielded the off-white pure solid compound.

*4-Nitrophenyl 3,4-Bis(hexyloxy)benzoate (**3a**).* $R_f$ = 0.55 (20% EtOAc−hexanes); white solid, mp: 95−97 °C; yield: 0.63 g (62%). IR (KBr pellet): $\nu_{max}$ in $cm^{-1}$ 2926, 2856, 2364, 1724, 1595, 1519, 1467, 1430, 1351, 1284, 1220, 1144, 1079, 953, 753; $^1H$ NMR ($CDCl_3$, 200 MHz): $\delta$ 8.32 (d, 2H, $J$ = 9.0 Hz, Ar), 7.82 (dd, 1H, $J$ = 2 Hz, $J$ = 8.4 Hz, Ar), 7.64 (d, 1H, $J$ = 1.8 Hz, Ar), 7.40 (d, 2H, $J$ = 9.2 Hz), 6.94 (d, 1H, $J$ = 8.6 Hz, Ar), 4.08 (m, 4H, $J$ = 6.4 Hz, 2 × $OCH_2$), 0.91−1.88 (m, 22H, 8 × $CH_2$, 2 × $CH_3$). $^{13}C$ NMR ($CDCl_3$, 100 MHz): 164.1, 156.0, 154.4, 148.8, 145.3, 125.2, 124.7, 122.7, 120.4, 114.7, 112, 69.4, 69.1, 31.5, 29.1, 29.0, 25.7, 22.6, 14.0. MS (FAB+): $m/z$ for $C_{25}H_{34}NO_6$ [M + 1], Calcd: 444.2. Found: 444.3. Anal. Calcd for $C_{25}H_{33}NO_6$: C, 67.7; H, 7.5; N, 3.16. Found: C, 68.1; H, 7.7; N, 3.3.

*4-Nitrophenyl 3,4-Bis(heptyloxy)benzoate (**3b**).* $R_f$ = 0.55 (20% EtOAc−hexanes); white solid, mp: 96−98 °C; yield: 0.7 g (65%). IR (KBr pellet): $\nu_{max}$ in $cm^{-1}$ 2924, 2849, 1723, 1595, 1519, 1467, 1429, 1352, 1283, 1220, 1144, 1079, 958, 753. $^1H$ NMR ($CDCl_3$, 400 MHz): $\delta$ 8.32 (d, 2H, $J$ = 8.8 Hz, Ar), 7.82 (d, 1H, $J$ = 8.4 Hz, Ar), 7.64 (s, 1H, Ar), 7.4 (d, 2H, $J$ = 8.8 Hz), 6.94 (d, 1H, $J$ = 8.4 Hz, Ar), 4.08 (m, 4H, $J$ = 6.4 Hz, 2 × $OCH_2$), 0.86−1.86 (m, 26H, 10 × $CH_2$, 2 × $CH_3$). $^{13}C$ NMR ($CDCl_3$, 100 MHz): 164.1, 156, 154.4, 148.8, 145.2, 125.2, 124.7, 122.7, 120.4, 114.5, 111.9, 69.4, 69.1, 31.8, 29.1, 29, 25.94, 25.90, 22.6, 14.1. MS (FAB+): $m/z$ for $C_{27}H_{37}NO_6$, Calcd: 471.26. Found: 471.2. Anal. Calcd for $C_{27}H_{37}NO_6$: C, 68.77; H, 7.91; N, 2.92. Found: C, 68.8; H, 7.6; N, 3.1.

*4-Nitrophenyl 3,4-Bis(octyloxy)benzoate (**3c**).* $R_f$ = 0.56 (20% EtOAc−hexanes); white solid, mp: 97−99 °C; yield: 0.81 g (70%). IR (KBr pellet): $\nu_{max}$ in $cm^{-1}$ 2924, 2850, 1723, 1595, 1519, 1430, 1352, 1285, 1220, 1144, 1079, 967, 753. $^1H$ NMR ($CDCl_3$, 200 MHz): $\delta$ 8.34 (d, 2H, $J$ = 9 Hz, Ar), 7.81 (dd, 1H, $J$ = 2.0 Hz, $J$ = 8.6 Hz, Ar), 7.64 (d, 1H, $J$ = 2 Hz, Ar), 7.41 (d, 2H, $J$ = 9.2 Hz), 6.94 (d, 1H, $J$ = 8.6 Hz, Ar), 4.08 (q, 4H, $J$ = 6.4 Hz, 2 × $OCH_2$), 0.86−1.91 (m, 30H, 12 × $CH_2$, 2 × $CH_3$). $^{13}C$ NMR ($CDCl_3$, 100 MHz): 164.1, 156.0, 154.4, 148.8, 145.3, 125.2, 124.7, 122.7, 120.4, 114.7, 112.0, 69.5, 69.1, 31.8, 29.3, 29.2, 29.16, 29, 25.99, 25.95, 22.7, 14.1. MS (FAB+): $m/z$ for $C_{29}H_{41}NO_6$, Calcd: 499.3. Found: 499. Anal. Calcd for $C_{29}H_{41}NO_6$: C, 69.71; H, 8.27; N, 2.8. Found: C, 69.5; H, 8.1; N, 2.9.

*4-Nitrophenyl 3,4-Bis(decyloxy)benzoate **3d**).* $R_f$ = 0.56 (20% EtOAc−hexanes); white solid, mp: 98−99 °C; yield: 0.92 g (72%). IR (KBr pellet): $\nu_{max}$ in $cm^{-1}$ 2919, 2848, 1723, 1595, 1519, 1429, 1353, 1283, 1221, 1145, 1080, 949, 753. $^1H$ NMR ($CDCl_3$, 200 MHz): $\delta$ 8.32 (d, 2H, $J$ = 9 Hz, Ar), 7.81 (dd, 1H, $J$ = 1.8 Hz, $J$ = 8.4 Hz, Ar), 7.64 (d, 1H, $J$ = 2 Hz, Ar), 7.4 (d, 2H, $J$ = 9.2 Hz), 6.94 (d, 1H, $J$ = 8.6 Hz, Ar), 4.08 (q, 4H, $J$ = 6.4 Hz, 2 × $OCH_2$), 0.85−1.87 (m, 38H, 16 × $CH_2$, 2 × $CH_3$). $^{13}C$ NMR ($CDCl_3$, 100 MHz): 164.1, 156.0, 154.5, 148.8, 145.3, 125.2, 124.7, 122.7, 120.4, 114.7, 112, 69.5, 69.1, 31.9, 29.59, 29.56, 29.4, 29.36, 29.33, 29.2, 29, 26.0, 25.96, 22.7, 14.1; MS (FAB+): $m/z$ for $C_{33}H_{50}NO_6$ [M + 1], Calcd: 556.4. Found: 556.5. Anal. Calcd for $C_{33}H_{49}NO_6$: C, 71.32; H, 8.89; N, 2.52. Found: C, 71.4; H, 8.6; N, 2.8.

*4-Nitrophenyl 3,4-Bis(dodecyloxy)benzoate (**3e**).* $R_f$ = 0.58 (20% EtOAc−hexanes); white solid, mp: 100−102 °C; yield: 0.87 g, (62%). IR (KBr pellet): $\nu_{max}$ in $cm^{-1}$ 2918, 2848, 1724, 1593, 1519, 1430, 1353, 1284, 1220, 1145, 1080, 949, 753. $^1H$ NMR ($CDCl_3$, 200 MHz): $\delta$ 8.32 (d, 2H, $J$ = 9 Hz, Ar), 7.82 (dd, 1H, $J$ = 2 Hz, $J$ = 8 Hz, Ar), 7.64 (d, 1H, $J$ = 2 Hz, Ar), 7.4 (d, 2H, $J$ = 8 Hz), 6.94 (d, 1H, $J$ = 8 Hz, Ar), 4.1 (q, 4H, $J$ = 6 Hz, 2 × $OCH_2$), 0.85−1.85 (m, 46H, 20 × $CH_2$, 2 × $CH_3$). $^{13}C$ NMR ($CDCl_3$, 100 MHz): 164.1, 156.0, 154.5, 148.9, 145.3, 125.2, 124.7, 122.7, 120.4, 114.7, 112.0, 69.5, 69.1, 31.9, 29.7, 29.66, 29.59, 29.56, 29.38, 29.36, 29.33, 29.2, 29.0, 26.0, 25.96, 22.7, 14.1; MS (FAB+): $m/z$ for $C_{37}H_{58}NO_6$ [M + 1], Calcd: 612.4. Found: 612.4. Anal. Calcd for $C_{37}H_{57}NO_6$: C, 72.63; H, 9.39; N, 2.29. Found: C, 72.4; H, 9.41; N, 2.41.

*General Procedure for the Synthesis of 4-Aminophenyl 3,4-Bis(alkoxy)benzoate (**4a**−**e**).* To a solution of nitro compound (1 mmol) (**3a**−**e**) in dry THF (20 mL) was added 10% Pd−C (5 wt %); the solution was degassed and stirred at RT under hydrogen atmosphere (1 atm, balloon) for 2 h. The reaction mixture was filtered over a Celite bed, and the bed was repeatedly washed with THF. Upon evaporating the THF under reduced pressure from the combined filtrate, the desired product was obtained as an white/off-white solid in quantitative yield. The product was absolutely pure and was used as such for the next reaction.

*4-Aminophenyl 3,4-Bis(hexyloxy)benzoate (**4a**).* $R_f$ = 0.28 (30% EtOAc−hexanes); off-white solid, mp: 93−94 °C. IR (KBr pellet): $\nu_{max}$ in $cm^{-1}$ 3349, 2931, 2858, 2365, 1727, 1707, 1597, 1510, 1429, 1353, 1277, 1191, 1141, 1089, 960, 757, 653. $^1H$ NMR ($CDCl_3$, 400 MHz): $\delta$ 7.79 (dd, 1H, $J$ = 2 Hz, $J$ = 8.4 Hz, Ar), 7.65 (d, 1H, $J$ = 2 Hz, Ar), 6.98 (dd, 2H, $J$ = 2.1 Hz, $J$ = 8.7 Hz, Ar), 6.92 (d, 1H, $J$ = 8.5 Hz, Ar), 6.71 (dd, 2H, $J$ = 2.2 Hz, $J$ = 8.7 Hz, Ar), 4.07 (q, 4H, $J$ = 6.5 Hz, 2 × $OCH_2$), 3.64 (brs, 2H, $NH_2$), 0.85−1.85 (m, 22H, 8 × $CH_2$, 2 × $CH_3$). $^{13}C$ NMR ($CDCl_3$, 400 MHz): 165.6, 153.6, 148.6, 144.1, 143.3, 124.2, 122.4, 121.9, 115.7, 114.6, 111.9, 69.3, 69.1, 31.6, 29.1, 29.0, 25.67, 25.65, 22.6, 14.0. MS (FAB +): $m/z$ for $C_{25}H_{36}NO_4$ [M + 1], Calcd: 414.3. Found: 414.1. Anal. Calcd for $C_{25}H_{35}NO_4$: C, 72.61; H, 8.53; N, 3.39. Found: C, 72.5; H, 8.6; N, 3.5.

*4-Aminophenyl 3,4-Bis(heptyloxy)benzoate (**4b**).* $R_f$ = 0.28 (30% EtOAc−hexanes); off-white solid, mp: 81−82 °C. IR (KBr pellet): $\nu_{max}$ in $cm^{-1}$ 3349, 2926, 2856, 2365, 1726, 1706, 1598, 1509, 1429, 1291, 1190, 1011, 960, 757, 652. $^1H$ NMR ($CDCl_3$, 400 MHz): $\delta$ 7.79 (dd, 1H, $J$ = 2 Hz, 8.4 Hz, Ar), 7.65 (d, 1H, $J$ = 2 Hz, Ar), 6.98 (d, 2H, $J$ = 12.0 Hz, Hz, Ar), 6.91 (d, 1H, $J$ = 8.5 Hz, Ar), 6.71 (d, 2H, $J$ = 12.2 Hz, Ar), 4.07 (q, 4H, $J$ = 6.48 Hz, 2 × $OCH_2$), 3.64 (brs, 2H, $NH_2$), 0.87−1.88 (m, 26H, 10 × $CH_2$, 2 × $CH_3$). $^{13}C$ NMR ($CDCl_3$, 100 MHz): 165.6, 153.6, 148.6, 144.1, 143.3, 124.2, 122.4, 121.9, 115.7, 114.6, 111.9, 69.3, 69.1, 31.8, 29.2, 29.1, 26, 25.9, 22.6, 14.0. MS (FAB +): $m/z$ for $C_{27}H_{39}NO_4$, Calcd: 441.3. Found: 441. Anal. Calcd for $C_{27}H_{39}NO_4$: C, 73.43; H, 8.9; N, 3.17. Found: C, 73.5; H, 8.71; N, 3.21.

*4-Aminophenyl 3,4-Bis(octyloxy)benzoate (**4c**).* $R_f$ = 0.27 (30% EtOAc−hexanes); off-white solid, mp: 74−75 °C. IR (KBr pellet): $\nu_{max}$ in $cm^{-1}$ 2923, 2851, 1730, 1696, 1598, 1512, 1428, 1279, 1090, 1014, 864, 754, 512. $^1H$ NMR ($CDCl_3$, 400 MHz): $\delta$ 7.79 (dd, 1H, $J$ = 4 Hz, $J$ = 8 Hz, Ar), 7.65 (d, 1H, $J$ = 4 Hz, Ar), 6.98 (d, 1H, $J$ = 12 Hz, Ar), 6.91 (d, 1H, $J$ = 12 Hz, Ar), 6.70 (d, 2H, $J$ = 12 Hz, Ar), 4.08 (q, 4H, $J$ = 8 Hz, 2 × $OCH_2$), 3.64 (s, 2H, $NH_2$), 0.87−1.89 (m, 30H, 12 × $CH_2$, 2 × $CH_3$). $^{13}C$ NMR ($CDCl_3$, 100 MHz): 165.6, 153.6, 148.6, 144.1, 143.3, 124.2, 122.4, 121.9, 115.7, 114.7, 112.0, 69.3, 69.1, 31.8, 29.2, 29.1, 25.94, 25.9, 22.6, 14.1. MS (FAB+): $m/z$ for $C_{29}H_{44}NO_4$ [M + 1], Calcd: 470.4. Found: 470.2. Anal. Calcd for $C_{29}H_{43}NO_4$: C, 74.16; H, 9.23; N, 2.98. Found: C, 74.3; H, 9.5; N, 3.1.

*4-Aminophenyl 3,4-Bis(decyloxy)benzoate (**4d**).* $R_f$ = 0.29 (30% EtOAc−hexanes); off-white solid, mp: 73−74 °C. IR (KBr pellet): $\nu_{max}$ in $cm^{-1}$ 3342, 2921, 2851, 1728, 1695, 1596, 1512, 1428, 1278, 1085, 1013, 760, 512. $^1H$ NMR ($CDCl_3$, 400 MHz): $\delta$ 7.79 (dd, 1H, $J$ = 4 Hz, $J$ = 8 Hz, Ar), 7.65 (d, 1H, $J$ = 4 Hz, Ar), 6.98 (d, 2H, $J$ = 12 Hz, Ar), 6.91 (d, 1H, $J$ = 12 Hz, Ar), 6.70 (d, 2H, $J$ = 12 Hz, Ar), 4.08 (q, 4H, $J$ = 8 Hz, 2 × $OCH_2$), 3.64 (brs, 2H, $NH_2$), 0.86−1.89 (m, 38H, 16 × $CH_2$, 2 × $CH_3$). $^{13}C$ NMR ($CDCl_3$, 100 MHz): 165.6, 153.7, 148.6, 144.1, 143.3, 124.2, 122.4, 121.9, 115.7, 114.7, 112.0, 69.4, 69.1, 31.9, 29.6, 29.56, 29.4, 29.3, 29.2, 29.1, 26, 25.96, 22.67, 14.1. MS (FAB+): $m/z$ for $C_{33}H_{52}NO_4$ [M + 1], Calcd: 526.4. Found: 526. Anal. Calcd for $C_{33}H_{51}NO_4$: C, 75.39; H, 9.78; N, 2.66. Found: C, 75.6; H, 9.9; N, 2.8.

*4-Aminophenyl 3,4-Bis(dodecyloxy)benzoate (**4e**).* $R_f$ = 0.28 (30% EtOAc−hexanes); off-white solid, mp: 70−71 °C. IR (KBr pellet): $\nu_{max}$ in $cm^{-1}$ 2920, 2850, 1716, 1594, 1515, 1471, 1275, 1079, 1006, 862, 762, 514. $^1H$ NMR ($CDCl_3$, 200 MHz): $\delta$ 7.79 (dd, 1H, $J$ = 2 Hz, 8.4 Hz, Ar), 7.65 (d, 1H, $J$ = 2 Hz, Ar), 6.89−7 (m, 3H, Ar), 6.71 (d, 2H, $J$ = 8.8 Hz, Ar), 4.02 −4.11 (m, 4H, 2 × $OCH_2$), 3.64 (bs, 2H, $NH_2$), 0.85−1.84 (m, 46H, 20 × $CH_2$, 2 × $CH_3$). $^{13}C$ NMR ($CDCl_3$, 100 MHz): 165.6, 153.7, 148.6, 144.1, 143.3, 124.2, 122.4, 121.9, 115.7, 114.7, 112.0, 69.4, 69.1, 31.9, 29.68, 29.65, 29.6, 29.40, 29.35, 29.2, 29.1, 26.0, 25.96, 22.7, 14.1. MS (FAB+): $m/z$ for $C_{37}H_{59}NO_4$, Calcd: 581.44. Found: 581.3. Anal. Calcd for $C_{37}H_{59}NO_4$: C, 76.37; H, 10.22; N, 2.41. Found: C, 76.5; H, 10.4; N, 2.5.


dx.doi.org/10.1021/jo302332u | J. Org. Chem. 2013, 78, 527−544

*General Procedure for the Synthesis of the **DLT-n** Series of Discotic Compounds.* A mixture of triformylphloroglucinol (0.168 g, 0.8 mmol, 1 equiv), 4-aminophenyl 3,4-bis(alkoxy)benzoate (5.4 mmol, 6.75 equiv) (**4a–e**) and absolute ethanol (25 mL) was heated to reflux for 2 h with vigorous stirring under nitrogen atmosphere. The pale yellow solid that separated upon cooling the reaction mixture was collected by filtration, repeatedly washed with hot ethanol, and air-dried. The crude product was further purified by repeated recrystallizations in a mixture of absolute ethanol–dichloromethane (9:1) until a constant isotropic phase transition temperature was obtained.

***DLT-6***. $R_f$ = 0.45 (30% EtOAc–hexanes); yellow solid, yield: 0.69 g (62%). UV–vis: $\lambda_{max}$ = 401.5 nm, $\varepsilon = 7.9 \times 10^4$ L mol$^{-1}$ cm$^{-1}$. IR (KBr pellet): $\nu_{max}$ in cm$^{-1}$ 2958, 2872, 1732, 1617, 1590, 1515, 1456, 1427, 1274, 1189, 1134, 1014, 868, 754. $^1$H NMR ($CDCl_3$, 400 MHz): $\delta$ 13.46 (d, $J$ = 12.8 Hz, =CNH), 13.42 (d, $J$ = 13.2 Hz, =CNH), 13.04 (d, $J$ = 13.2 Hz, =CNH) – these resonances are due to three amine protons, 8.69–8.80 (m, 3H, =CHN), 7.78–7.81 (dd, 3H, $J$ = 2 Hz, 2 Hz, Ar), 7.65 (d, 3H, $J$ = 2 Hz, Ar), 7.25–7.37 (m, 12H, Ar), 6.94 (d, 3H, $J$ = 8.4 Hz, Ar), 4.05–4.10 (m, 12H, 6 × $OCH_2$), 0.89–1.88 (m, 66H, 24 × $CH_2$, 6 × $CH_3$). $^{13}$C NMR ($CDCl_3$, 100 MHz): 188.2, 185.4, 182.4, 164.9, 154.0, 150.2, 149.7, 149.4, 148.7, 148.6, 136.7, 124.4, 123.4, 121.2, 118.6, 118.5, 114.6, 112.0, 107.1, 107.0, 106.8, 69.4, 69.1, 31.6, 29.1, 29.02, 25.7, 25.6, 22.6, 14.1. MS (FAB+): $m/z$ for $C_{84}H_{105}N_3O_{15}$, Calcd: 1395.8. Found: 1396. Anal. Calcd for $C_{84}H_{105}N_3O_{15}$: C, 72.23; H, 7.58; N, 3.01. Found: C, 72.4; H, 7.7; N, 2.8.

***DLT-7***. $R_f$ = 0.45 (30% EtOAc–hexanes); yellow solid, yield: 0.84 g (71%). UV–vis: $\lambda_{max}$ = 402.9 nm, $\varepsilon = 10.4 \times 10^4$ L mol$^{-1}$ cm$^{-1}$. IR (KBr pellet): $\nu_{max}$ in cm$^{-1}$ 2925, 1734, 1618, 1590, 1516, 1458, 1272, 1202, 868, 754. $^1$H NMR ($CDCl_3$, 400 MHz): $\delta$ 13.47 (d, $J$ = 12.8 Hz, =CNH), 13.42 (d, $J$ = 13.2 Hz, =CNH), 13.05 (d, $J$ = 13.2 Hz, =CNH) – these resonances are due to three amine protons, 8.67–8.82 (m, 3H, =CHN), 7.77–7.81 (dd, 3H, $J$ = 2 Hz, 2 Hz, Ar), 7.65 (d, 3H, $J$ = 1.6 Hz, Ar), 7.25–7.38 (m, 12H, Ar), 6.92 (d, 3H, $J$ = 8.4 Hz, Ar), 4.05–4.10 (m, 12H, 6 × $OCH_2$), 0.88–1.90 (m, 78H, 30 × $CH_2$, 6 × $CH_3$). $^{13}$C NMR ($CDCl_3$, 100 MHz): 188.3, 185.5, 182.4, 164.9, 154.0, 149.4, 148.7, 148.65, 136.7, 124.4, 123.4, 121.2, 118.6, 118.5, 114.7, 112.0, 107.1, 107.0, 106.8, 69.4, 69.1, 31.8, 29.2, 29.1, 26.0, 25.9, 22.6 14.1. MS (FAB+): $m/z$ for $C_{90}H_{117}N_3O_{15}$, Calcd: 1479.8. Found: 1480. Anal. Calcd for $C_{90}H_{117}N_3O_{15}$: C, 72.99; H, 7.96; N, 2.84. Found: C, 73.4; H, 7.6; N, 2.9.

***DLT-8***. $R_f$ = 0.45 (30% EtOAc–hexanes); yellow solid, yield: 0.81 g (65%). UV–vis: $\lambda_{max}$ = 401.21 nm, $\varepsilon = 8.2 \times 10^4$ L mol$^{-1}$ cm$^{-1}$. IR (KBr pellet): $\nu_{max}$ in cm$^{-1}$ 2924, 2854, 1734, 1653, 1617, 1590, 1516, 1457, 1271, 1188, 868, 753. $^1$H NMR ($CDCl_3$, 400 MHz): $\delta$ 13.5 (d, $J$ = 12.8 Hz, =CNH), 13.46 (d, $J$ = 13.2 Hz, =CNH), 13.01 (d, $J$ = 13.2 Hz, =CNH) – these resonances are due to three amine protons, 8.74–8.84 (m, 3H, =CHN), 7.77–7.81 (dd, 3H, $J$ = 1.6 Hz, 1.6 Hz, Ar), 7.65 (d, 3H, $J$ = 1.6 Hz, Ar), 7.25–7.37 (m, 12H, Ar), 6.92 (d, 3H, $J$ = 8.8 Hz, Ar), 4.05–4.10 (m, 12H, 6 × $OCH_2$), 0.87–1.89 (m, 90H, 36 × $CH_2$, 6 × $CH_3$). $^{13}$C NMR ($CDCl_3$, 100 MHz): 188.2, 185.4, 182.4, 164.9, 154, 150.2, 149.7, 149.4, 148.7, 148.6, 136.7, 124.4, 123.3, 121.2, 118.6, 118.5, 114.7, 112.0, 107.1, 107.0, 106.8, 69.4, 69.1, 31.8, 29.34, 29.25, 29.2, 29.1, 26.0, 25.97, 22.7, 14.1. MS (FAB+): $m/z$ for $C_{96}H_{130}N_3O_{15}$ [M + 1], Calcd: 1564.95. Found: 1565.7. Anal. Calcd for $C_{96}H_{129}N_3O_{15}$: C, 73.67; H, 8.31; N, 2.68. Found: C, 73.4; H, 8.5; N, 2.6.

***DLT-10***. $R_f$ = 0.45 (30% EtOAc–hexanes); yellow solid, yield: 0.93 g (67%). UV–vis: $\lambda_{max}$ = 402.12 nm, $\varepsilon = 9.2 \times 10^4$ L mol$^{-1}$ cm$^{-1}$. IR (KBr pellet): $\nu_{max}$ in cm$^{-1}$ 2921, 2852, 1732, 1621, 1590, 1515, 1455, 1428, 1272, 1189, 1140, 868, 754. $^1$H NMR ($CDCl_3$, 400 MHz): $\delta$ 13.47 (d, $J$ = 12.8 Hz, =CNH), 13.43 (d, $J$ = 13.2 Hz, =CNH), 13.04 (d, $J$ = 13.2 Hz, =CNH) – these resonances are due to three amine protons, 8.69–8.81 (m, 3H, =CHN), 7.79–7.81 (dd, 3H, $J$ = 1.6 Hz, 1.6 Hz, Ar), 7.65 (d, 3H, $J$ = 1.6 Hz, Ar), 7.25–7.40 (m, 12H, Ar), 6.92 (d, 3H, $J$ = 8.8 Hz, Ar), 4.05–4.09 (m, 12H, 6 × $OCH_2$), 0.86–1.90 (m, 114H, 48 × $CH_2$, 6 × $CH_3$). $^{13}$C NMR ($CDCl_3$, 100 MHz): 188.2, 185.4, 182.4, 164.9, 154, 150.2, 149.7, 149.4, 148.7, 148.6, 136.7, 124.4, 123.4, 121.2, 118.6, 118.5, 114.7, 112, 107.1, 107.0, 106.8, 69.4, 69.1, 31.9, 29.6, 29.56, 29.4, 29.3, 29.2, 29.1, 26.0, 25.97, 22.67, 14.1. MS (FAB+): $m/z$ for $C_{108}H_{154}N_3O_{15}$ [M + 1], Calcd: 1733.2. Found: 1733.1. Anal. Calcd for $C_{108}H_{153}N_3O_{15}$: C, 74.83; H, 8.9; N, 2.42. Found: C, 75; H, 9; N, 2.5.

***DLT-12***. $R_f$ = 0.45 (30% EtOAc–hexanes); yellow solid, yield: 1.03 g (68%). UV–vis: $\lambda_{max}$ = 401.30 nm, $\varepsilon = 8.8 \times 10^4$ L mol$^{-1}$ cm$^{-1}$. IR (KBr pellet): $\nu_{max}$ in cm$^{-1}$ 2922, 2851, 1730, 1620, 1590, 1515, 1457, 1428, 1272, 1140, 867, 753. $^1$H NMR ($CDCl_3$, 400 MHz): $\delta$ 13.48 (d, $J$ = 12.8 Hz, =CNH), 13.43 (d, $J$ = 13.2 Hz, =CNH), 13.05 (d, $J$ = 12.8 Hz, =CNH) – these resonances are due to three amine protons, 8.70–8.82 (m, 3H, =CHN), 7.79–7.81 (dd, 3H, $J$ = 1.6 Hz, 1.6 Hz, Ar), 7.65 (d, 3H, $J$ = 1.6 Hz, Ar), 7.26–7.38 (m, 12H, Ar), 6.92 (d, 3H, $J$ = 8.8 Hz, Ar), 4.05–4.1 (m, 12H, 6 × $OCH_2$), 0.86–1.90 (m, 138H, 60 × $CH_2$, 6 × $CH_3$). $^{13}$C NMR ($CDCl_3$, 100 MHz): 188.2, 185.5, 182.4, 164.9, 154, 149.4, 148.7, 148.7, 136.7, 124.4, 123.4, 121.2, 118.6, 118.5, 114.7, 112.0, 107.1, 107, 106.8, 69.4, 69.1, 31.9, 29.7, 29.65, 29.62, 29.4, 29.2, 29.1, 26.01, 25.98, 22.7, 14.1. MS (FAB+): $m/z$ for $C_{120}H_{178}N_3O_{15}$ [M + 1], Calcd: 1901.3. Found: 1901.3. Anal. Calcd for $C_{120}H_{177}N_3O_{15}$: C, 75.79; H, 9.38; N, 2.21. Found: C, 75.4; H, 9.7; N, 2.3.

*Synthesis of Ethyl 3,4,5-Trihydroxybenzoate (**5**).* A mixture of gallic acid (5 g, 29.4 mmol), ethanol (50 mL), and a few drops of conc $H_2SO_4$ was refluxed for 5 h. Excess of the solvent was removed in vacuo; the reaction mixture was poured into cold water and extracted with ethyl acetate repeatedly. Combined extracts were washed with 10% $NaHCO_3$, water, and brine, dried over anhyd $Na_2SO_4$, and concentrated. The crude solid was recrystallized with ethanol to get a white solid with a yield of 80%. $R_f$ = 0.79 in 20% EtOAc-hexanes; white solid; mp 152–153 °C (lit 152–154 °C); yield: 5.53g 95%; IR (KBr pellet): $\nu_{max}$ in cm$^{-1}$ 3420, 2930, 1728, 1230; $^1$H NMR ($CDCl_3$, 400 MHz): $\delta$ 9.8 (s, 3H, 3 × OH), 7.47 (m, 2H, Ar), 4.35 (t, $J$ = 7 Hz, 2H, 2 × $OCH_2$) and 1.54 (t, $J$ = 6.9 Hz, 3H, 1 × $CH_3$); MS (FAB+): $m/z$ for $C_9H_{10}O_5$, Calculated: 198.05, Found: 198.

*General Procedure for the Synthesis of Ethyl 3,4,5-Trialkoxy Benzoates (**6a–f**).* A mixture of ethyl 3,4,5-trihydroxybenzoate (**5**) (2 g, 10.1 mmol, 1equiv), anhyd $K_2CO_3$ (8.4 g, 60.6 mmol, 6.6 equiv), and the appropriate *n*-bromoalkane (33.3 mmol, 3.3 equiv) was taken in dry DMF (20 mL) and heated at 80 °C for 12 h under nitrogen atmosphere. The reaction was cooled, poured into ice cold water, and extracted with $CH_2Cl_2$ several times. The combined extracts were washed with water and brine, dried over anhyd $Na_2SO_4$, and concentrated. The crude product was purified by column chromatography on neutral alumina. Elution with hexanes followed by 5–10% ethyl acetate–hexanes yielded the desired product. Yields of these compounds were in the range 70–84%.

*Ethyl 3,4,5-Tributoxybenzoate (**6a**).* $R_f$ = 0.6 (10% EtOAc–hexanes); colorless liquid, yield: 2.59 g (70%). IR (KBr pellet): $\nu_{max}$ in cm$^{-1}$ 2959, 2934, 2872, 1716, 1587, 1499, 1463, 1430, 1331, 1211, 1110, 766, 618. $^1$H NMR ($CDCl_3$, 200 MHz): $\delta$ 7.26 (s, 2H, Ar), 4.36 (q, 2H, $J$ = 8 Hz, $COOCH_2$), 4.03 (t, 6H, $J$ = 6.0 Hz, 3 × $OCH_2$), 0.92–1.87 (m, 24H, 6 × $CH_2$,4 × $CH_3$). MS (FAB+): $m/z$ for $C_{21}H_{34}O_5$, Calcd: 366.3. Found: 366.8. Anal. Calcd for $C_{21}H_{34}O_5$: C, 68.82; H, 9.35. Found: C, 68.7; H, 9.4.

*Ethyl 3,4,5-Tris(pentyloxy)benzoate (**6b**).* $R_f$ = 0.58 (10% EtOAc–hexanes); colorless liquid,[24] yield: 2.9 g (70%). IR (KBr pellet): $\nu_{max}$ in cm$^{-1}$ 2956, 2871, 1718, 1587, 1499, 1466, 1430, 1332, 1217, 1109, 765, 620. $^1$H NMR ($CDCl_3$, 200 MHz): $\delta$ 7.26 (s, 2H, Ar), 4.36 (q, 2H, $J$ = 7 Hz, $COOCH_2$), 4.02 (t, 6H, $J$ = 6.4 Hz, 3 × $OCH_2$), 0.90–1.89 (m, 30H, 9 × $CH_2$, 4 × $CH_3$). MS (FAB+): $m/z$ for $C_{24}H_{40}O_5$, Calcd: 408.3. Found: 408.9. Anal. Calcd for $C_{24}H_{40}O_5$: C, 70.55; H, 9.87. Found: C, 70.8; H, 9.7.

*Ethyl 3,4,5-Tris(hexyloxy)benzoate (**6c**).* $R_f$ = 0.57 (10% EtOAc–hexanes); colorless liquid,[24] yield: 3.27 g (72%). IR (KBr pellet): $\nu_{max}$ in cm$^{-1}$ 2931, 2859, 1718, 1586, 1500, 1467, 1429, 1332, 1215, 1112, 1033, 766, 617. $^1$H NMR ($CDCl_3$, 200 MHz): $\delta$ 7.26 (s, 2H, Ar), 4.36 (q, 2H, $J$ = 6 Hz, $COOCH_2$), 4.02 (t, 6H, $J$ = 6.0 Hz, 3 × $OCH_2$), 0.87–1.88 (m, 36H, 12 × $CH_2$, 4 × $CH_3$). MS (FAB+): $m/z$ for $C_{27}H_{46}O_5$, Calcd: 450.3. Found: 450.3. Anal. Calcd for $C_{27}H_{46}O_5$: C, 71.96; H, 10.29. Found: C, 71.5; H, 10.5.


dx.doi.org/10.1021/jo302332u | *J. Org. Chem.* 2013, 78, 527–544

*Ethyl 3,4,5-Tris(heptyloxy)benzoate (**6d**).* $R_f$ = 0.6 (30% EtOAc–hexanes); colorless liquid,[24] yield: 3.7 g (70%). IR (KBr pellet): $\nu_{max}$ in $cm^{-1}$ 2930, 2858, 1718, 1586, 1499, 1466, 1430, 1332, 1215, 1112, 1032, 764, 617. $^1H$ NMR ($CDCl_3$, 200 MHz): $\delta$ 7.25 (s, 2H, Ar), 4.35 (q, 2H, $J$ = 7 Hz, $COOCH_2$), 4.03 (t, 6H, $J$ = 6.4 Hz, 3 × $OCH_2$), 0.86–1.88 (m, 42H, 15 × $CH_2$, 4 × $CH_3$). MS (FAB+): $m/z$ for $C_{30}H_{52}O_5$, Calcd: 492.4. Found: 492.2. Anal. Calcd for $C_{30}H_{52}O_5$: C, 73.13; H, 10.64. Found: C, 73.5; H, 10.4.

*Ethyl 3,4,5-Tris(octyloxy)benzoate (**6e**).* $R_f$ = 0.59 (10% EtOAc–hexanes); colorless liquid,[24] yield: 3.8 g (74%). IR (KBr pellet): $\nu_{max}$ in $cm^{-1}$ 2926, 2856, 1719, 1587, 1500, 1467, 1430, 1333, 1217, 1113, 1034, 765, 610. $^1H$ NMR ($CDCl_3$, 200 MHz): $\delta$ 7.26 (s, 2H, Ar), 4.35 (q, 2H, $J$ = 7 Hz, $COOCH_2$), 4.02 (t, 6H, $J$ = 6.4 Hz, 3 × $OCH_2$), 0.85–1.88 (m, 48H, 18 × $CH_2$, 4 × $CH_3$). MS (FAB+): $m/z$ for $C_{33}H_{58}O_5$, Calcd: 534.4. Found: 534.7. Anal. Calcd for $C_{33}H_{58}O_5$: C, 74.11; H, 10.93. Found: C, 73.9; H, 10.81.

*Ethyl 3,4,5-Tris(decyloxy)benzoate (**6f**).* $R_f$ = 0.58 (10% EtOAc–hexanes); colorless viscous liquid,[24] yield: 4.4 g (70%). IR (KBr pellet): $\nu_{max}$ in $cm^{-1}$ 2925, 2854, 1719, 1587, 1499, 1429, 1332, 1215, 1115, 1034, 765, 612. $^1H$ NMR ($CDCl_3$, 200 MHz): $\delta$ 7.26 (s, 2H, Ar), 4.35 (q, 2H, $J$ = 6.6 Hz, $COOCH_2$), 4.01 (t, 6H, $J$ = 6.4 Hz, 3 × $OCH_2$), 0.85–1.88 (m, 60H, 24 × $CH_2$, 4 × $CH_3$). MS (FAB+): $m/z$ for $C_{39}H_{70}O_5$, Calcd: 618.5. Found: 618.7. Anal. Calcd for $C_{39}H_{70}O_5$: C, 75.68; H, 11.4. Found: C, 75.8; H, 11.6.

*General Procedure for the Synthesis of 3,4,5-Tri(alkoxy)benzoic Acids (**7a–f**).* To a well-stirred solution of ethyl 3,4,5-tris(*n*-alkoxy)benzoate (8.6 mmol, 1 equiv) in ethanol (50 mL), an aqueous solution of NaOH (15%) (0.7 g, 17.2 mmol, 2 equiv) (20 mL) was added, and the resultant reaction mixture was heated to reflux for 6 h. It may be noted here that frothing during the heating of the reaction mixture was controlled by addition of water. Excess of ethanol was removed under vacuum, and the residue was poured on to crushed ice with vigorous stirring. The cold solution was acidified with conc HCl and extracted with EtOAc repeatedly. The extracts were mixed, dried over anhyd $Na_2SO_4$, and concentrated. A crude compound collected was suspended in hot hexanes and stirred for 5 min and filtered to remove the traces of unreacted starting material. The off-white solid thus obtained was purified by repeated recrystallization from ethanol until a constant melting point was obtained.

*3,4,5-Tributoxybenzoic acid (**7a**).* $R_f$ = 0.25 (50% EtOAc–hexanes); off white solid, mp: 72–73 °C (lit.[25f] mp: 70 °C); yield: 2.5 g (85%). IR (KBr pellet): $\nu_{max}$ in $cm^{-1}$ 2958, 2871, 1686, 1590, 1467, 1433, 1386, 1331, 1228, 1131, 1116, 866, 768, 542. $^1H$ NMR ($CDCl_3$, 200 MHz): $\delta$ 7.32 (s, 2H, Ar), 4–4.1 (t, 6H, 3 × $OCH_2$), 0.93–1.88 (m, 21H, 6 × $CH_2$, 3 × $CH_3$). MS (FAB+): $m/z$ for $C_{19}H_{30}O_5$, Calcd: 338.2. Found: 338.8. Anal. Calcd for $C_{19}H_{30}O_5$: C, 67.43; H, 8.93. Found: C, 67.8; H, 8.8.

*3,4,5-Tris(pentyloxy)benzoic acid (**7b**).* $R_f$ = 0.26 (50% EtOAc–hexanes); off-white solid, mp: 50–51 °C (lit.[25] mp: 49 °C); yield: 3 g (92%). IR (KBr pellet): $\nu_{max}$ in $cm^{-1}$ 2956, 2870, 1688, 1588, 1468, 1432, 1332, 1228, 1117, 766, 737, 541. $^1H$ NMR ($CDCl_3$, 200 MHz): $\delta$ 7.37 (s, 2H, Ar), 4.04–4.13 (t, 6H, 3 × $OCH_2$), 0.95–1.91 (m, 27H, 9 × $CH_2$, 3 × $CH_3$). MS (FAB+): $m/z$ for $C_{22}H_{36}O_5$, Calcd: 380.3. Found: 380.9. Anal. Calcd for $C_{22}H_{36}O_5$: C, 69.44; H, 9.54. Found: C, 69.2; H, 9.2.

*3,4,5-Tris(hexyloxy)benzoic acid (**7c**).* $R_f$ = 0.26 (50% EtOAc–hexanes); off-white solid, mp: 42–43 °C (lit.[25] mp: 39 °C); yield: 3.2 g (87%). IR (KBr pellet): $\nu_{max}$ in $cm^{-1}$ 2956, 2854, 1692, 1588, 1466, 1431, 1329, 1226, 1114, 768, 734, 545. $^1H$ NMR ($CDCl_3$, 200 MHz): $\delta$ 7.37 (s, 2H, Ar), 4.04–4.13 (t, 6H, 3 × $OCH_2$), 0.95–1.91 (m, 33H, 12 × $CH_2$, 3 × $CH_3$). MS (FAB+): $m/z$ for $C_{25}H_{42}O_5$, Calcd: 422.3. Found: 422.0. Anal. Calcd for $C_{25}H_{42}O_5$: C, 71.05; H, 10.02. Found: C, 71.25; H, 10.2.

*3,4,5-Tris(heptyloxy)benzoic acid (**7d**).* $R_f$ = 0.27 (50% EtOAc–hexanes); off-white solid, mp: 42–43 °C (lit.[25] mp: 42 °C); yield: 3.7 g (92%). IR (KBr pellet): $\nu_{max}$ in $cm^{-1}$ 2956, 2854, 1692, 1588, 1466, 1389, 1329, 1231, 1116, 766, 726, 547. $^1H$ NMR ($CDCl_3$, 200 MHz): $\delta$ 7.32 (s, 2H, Ar), 4.06–4.13 (t, 6H, 3 × $OCH_2$), 0.86–1.89 (m, 39H, 15 × $CH_2$, 3 × $CH_3$). MS (FAB+): $m/z$ for $C_{28}H_{48}O_5$, Calcd: 464.4. Found: 467.9. Anal. Calcd for $C_{28}H_{48}O_5$: C, 72.37; H, 10.41. Found: C, 72.5; H, 10.5.

*3,4,5-Tris(octyloxy)benzoic acid (**7e**).* $R_f$ = 0.27 (50% EtOAc–hexanes); off-white solid, mp: 55–56 °C (lit.[25] mp: 54 °C); yield: 3.8 g (88%). IR (KBr pellet): $\nu_{max}$ in $cm^{-1}$ 2922, 2849, 1587, 1466, 1433, 1392, 1330, 1229, 1115, 766, 720, 550. $^1H$ NMR ($CDCl_3$, 200 MHz): $\delta$ 7.32 (s, 2H, Ar), 3.99–4.1 (t, 6H, 3 × $OCH_2$), 0.85–1.89 (m, 45H, 18 × $CH_2$, 3 × $CH_3$). MS (FAB+): $m/z$ for $C_{31}H_{54}O_5$, Calcd: 506.4. Found: 506.5. Anal. Calcd for $C_{31}H_{54}O_5$: C, 73.47; H, 10.74. Found: C, 73.6; H, 10.8.

*3,4,5-Tris(decyloxy)benzoic acid (**7f**).* $R_f$ = 0.27 (50% EtOAc–hexanes); off-white solid, mp: 52–53 °C (lit.[25] mp: 54 °C); yield: 4.3 g (84%). IR (KBr pellet): $\nu_{max}$ in $cm^{-1}$ 2922, 2850, 1586, 1466, 1434, 1332, 1231, 1118, 864, 765, 539. $^1H$ NMR ($CDCl_3$, 200 MHz): $\delta$ 7.32 (s, 2H, Ar), 3.99–4.1 (t, 6H, 3 × $OCH_2$), 0.85–1.89 (m, 57H, 24 × $CH_2$, 3 × $CH_3$). MS (FAB+): $m/z$ for $C_{37}H_{66}O_5$, Calcd: 590.5. Found: 590.7. Anal. Calcd for $C_{37}H_{66}O_5$: C, 75.2; H, 11.26. Found: C, 74.9; H, 11.5.

*General Procedure for the Synthesis of 4-Nitrophenyl 3,4,5-Trialkoxybenzoates (**8a–f**).* A mixture of 3,4,5-tri(alkoxy)benzoic acid (**7a–f**) (2.3 mmol, 1 equiv) and 4-nitrophenol (0.32 g, 2.3 mmol, 1 equiv) was dissolved in dry THF (20 mL), degassed, and stirred under nitrogen atmosphere. To this solution was added a solution of DCC (0.71 g, 3.45 mmol, 1.5 equiv) and a catalytic amount of DMAP (0.015 g, 0.12 mmol, 0.05 equiv) in THF (10 mL). The reaction mixture was stirred at room temperature for 12 h under nitrogen atmosphere. The precipitated dicyclohexylurea was filtered off, and the combined filtrate was concentrated. The residue was dissolved in ethyl acetate, washed with 5% cold NaOH(aq) solution, water, and brine, dried over anhyd $Na_2SO_4$, and concentrated. The crude product was purified by column chromatography using silica gel (100–200). Elution with hexanes followed by 5% EtOAc–hexanes yielded the off-white solid compound.

*4-Nitrophenyl 3,4,5-Tributoxybenzoate (**8a**).* $R_f$ = 0.59 (20% EtOAc–hexanes); off-white solid, mp: 96–97 °C; yield: 0.64 g (60%). IR (KBr pellet): $\nu_{max}$ in $cm^{-1}$ 2959, 2874, 2362, 1738, 1592, 1524, 1462, 1434, 1338, 1334, 1246, 1186, 1162, 864, 780, 682. $^1H$ NMR ($CDCl_3$, 400 MHz): $\delta$ 8.32 (2H, d, $J$ = 9 Hz, Ar), 7.39–7.38 (m, 4H, Ar), 4.10–4.05 (m, 6H, 3 × $OCH_2$), 1.42–1.90 (m, 12H, 6 × $CH_2$), 0.94 (m, 9H, Hz, 3 × $CH_3$). $^{13}C$ NMR ($CDCl_3$, 100 MHz): 164.2, 155.9, 153.1, 145.4, 143.6, 125.3, 122.8, 108.7, 73.3, 69, 32.3, 31.3, 19.3, 19.1, 13.8. MS (FAB+): $m/z$ for $C_{25}H_{33}NO_7$, Calcd: 459.3. Found: 459.7. Anal. Calcd for $C_{25}H_{33}NO_7$: C, 65.34; H, 7.24; N, 3.05. Found: C, 65.62; H, 7.6; N, 2.9.

*4-Nitrophenyl 3,4,5-Tris(pentyloxy)benzoate (**8b**).* $R_f$ = 0.60 (20% EtOAc–hexanes); off-white solid, mp: 79–80 °C; yield: 0.71 g (62%). IR (KBr pellet): $\nu_{max}$ in $cm^{-1}$ 2956, 2871, 2361, 1737, 1592, 1523, 1469, 1432, 1336, 1334, 1187, 1162, 1114, 946, 860, 753, 582. $^1H$ NMR ($CDCl_3$, 200 MHz): $\delta$ 8.33 (2H, d, $J$ = 9.0 Hz, Ar) 7.37–7.41 (m, 4H, Ar), 4.01–4.11 (m, 6H, 3 × $OCH_2$), 1.42–1.92 (m, 18H, 9 × $CH_2$), 0.94 (t, 9H, $J$ = 6.8 Hz, 3 × $CH_3$). $^{13}C$ NMR ($CDCl_3$, 100 MHz): 164.1, 155.9, 153.1, 145.3, 143.5, 125.2, 122.7, 108.7, 73.6, 69.3, 30, 28.9, 28.2, 28.1, 22.5, 22.4, 14.0. MS (FAB+): $m/z$ for $C_{28}H_{39}NO_7$, Calcd: 501.3. Found: 501. Anal. Calcd for $C_{28}H_{39}NO_7$: C, 67.04; H, 7.84; N, 2.79. Found: C, 67.5; H, 7.4; N, 2.5.

*4-Nitrophenyl 3,4,5-Tris(hexyloxy)benzoate (**8c**).* $R_f$ = 0.60 (20% EtOAc–hexanes); off-white solid, mp: 59–60 °C; yield: 0.74 g (59%). IR (KBr pellet): $\nu_{max}$ in $cm^{-1}$ 2928, 2858, 2361, 1737, 1592, 1524, 1432, 1336, 1188, 1114, 944, 860, 738, 579. $^1H$ NMR ($CDCl_3$, 200 MHz): $\delta$ 8.33 (d, 2H, $J$ = 9.2 Hz, Ar), 7.37–7.41 (m, 4H, Ar), 4.03–4.10 (m, 6H, 3 × $OCH_2$), 1.34–1.86 (m, 24H, 12 × $CH_2$), 0.87–0.91 (m, 9H, 3 × $CH_3$). $^{13}C$ NMR ($CDCl_3$, 100 MHz): 164.2, 155.9, 153.1, 145.4, 143.6, 125.3, 122.7, 108.7, 73.7, 69.3, 31.8, 31.5, 30.3, 29.2, 25.7, 25.69, 22.7, 22.6, 18.1, 14.0. MS (FAB+): $m/z$ for $C_{31}H_{45}NO_7$, Calcd: 543.3. Found: 544.0. Anal. Calcd for $C_{31}H_{45}NO_7$: C, 68.48; H, 8.34; N, 2.58. Found: C, 68.5; H, 8.3; N, 2.7.

*4-Nitrophenyl 3,4,5-Tris(heptyloxy)benzoate (**8d**).* $R_f$ = 0.61 (20% EtOAc–hexanes); off-white solid, mp: 53–54 °C; yield: 0.92 g (68%). IR (KBr pellet): $\nu_{max}$ in $cm^{-1}$ 2931, 2856, 1738, 1592, 1520, 1430, 1337, 1186, 1115, 940, 862, 753, 683. $^1H$ NMR ($CDCl_3$, 200 MHz): $\delta$


dx.doi.org/10.1021/jo302332u | J. Org. Chem. 2013, 78, 527–544

8.33 (2H, d, $J$ = 9.2 Hz, Ar) 7.37−7.41 (m, 4H, Ar), 4.03−4.10 (m, 6H, 3 × $OCH_2$), 1.30−1.83 (m, 30H, 15 × $CH_2$), 0.87−0.91 (m, 9H, 3 × $CH_3$). $^{13}$C NMR ($CDCl_3$, 100 MHz): 164.2, 155.9, 153.1, 145.4, 143.6, 125.3, 122.8, 108.7, 73.7, 69.4, 31.9, 31.8, 30.4, 29.3, 29.2, 29.1, 26, 25.99, 22.7, 22.6, 14.1. MS (FAB+): $m/z$ for $C_{34}H_{52}NO_7$ [M + 1], Calcd: 586.4. Found: 586.3. Anal. Calcd for $C_{34}H_{51}NO_7$: C, 69.71; H, 8.78; N, 2.39. Found: C, 69.5; H, 8.5; N, 2.6.

*4-Nitrophenyl 3,4,5-Tris(octyloxy)benzoate (**8e**).* $R_f$ = 0.62 (20% EtOAc−hexanes); off-white solid, mp: 41−42 °C; yield: 0.94 g (65%). IR (KBr pellet): $\nu_{max}$ in cm$^{-1}$ 2923, 2853, 1742, 1593, 1530, 1433, 1338, 1188, 1122, 938, 857, 747, 684. $^1$H NMR ($CDCl_3$, 200 MHz): $\delta$ 8.34 (2H, d, $J$ = 9.0 Hz, Ar) 7.37−7.41 (m, 4H, Ar), 4.03−4.10 (m, 6H, 3 × $OCH_2$), 1.29−1.86 (m, 36H, 18 × $CH_2$), 0.87−0.90 (m, 9H, 3 × $CH_3$). $^{13}$C NMR ($CDCl_3$, 100 MHz): 164.2, 155.9, 153.1, 145.4, 143.6, 125.3, 122.7, 108.7, 73.7, 69.4, 31.9, 31.8, 30.4, 29.5, 29.34, 29.28, 26.1, 26.04, 22.7, 14.1. MS (FAB+): $m/z$ for $C_{37}H_{57}NO_7$, Calcd: 627.4. Found: 627.7. Anal. Calcd for $C_{37}H_{57}NO_7$: C, 70.78; H, 9.15; N, 2.23. Found: C, 70.6; H, 9.4; N, 2.4.

*4-Nitrophenyl 3,4,5-Tris(decyloxy)benzoate (**8f**).* $R_f$ = 0.63 (20% EtOAc−hexanes); off-white solid, mp: 56−57 °C; yield: 1.1 g (69%). IR (KBr pellet): $\nu_{max}$ in cm$^{-1}$ 2931, 2856, 1738, 1592, 1520, 1431, 1337, 1240, 1187, 1115, 939, 860, 752, and 694. $^1$H NMR ($CDCl_3$, 200 MHz): $\delta$ 8.32 (2H, d, $J$ = 8 Hz, Ar) 7.38−7.40 (m, 4H, Ar), 4.03−4.11 (m, 6H, 3 × $OCH_2$), 1.27−1.87 (m, 48H, 24 × $CH_2$), 0.87−0.90 (m, 9H, 3 × $CH_3$). $^{13}$C NMR ($CDCl_3$, 100 MHz): 164.1, 155.9, 153.1, 145.4, 143.7, 125.2, 122.7, 108.8, 73.7, 69.4, 31.9, 30.3, 29.7, 29.65, 29.61, 29.57, 29.4, 29.33, 29.29, 26.1, 22.7, 14.1. MS (FAB+): $m/z$ for $C_{43}H_{69}NO_7$, Calcd: 711.5. Found: 711.7. Anal. Calcd for $C_{43}H_{69}NO_7$: C, 72.54; H, 9.77; N, 1.97. Found: C, 72.8; H, 9.5; N, 2.2.

*General Procedure for the Synthesis of 4-Aminophenyl 3,4,5-Trialkoxybenzoates (**9a−f**).* To a solution of 4-nitrophenyl 3,4,5-trialkoxybenzoates (**8a−f**) (1 mmol) in dry THF (20 mL) was added 10% Pd−C (5 wt %); the mixture was degassed and stirred under hydrogen atmosphere (1 atm, balloon) for 3 h. The reaction mixture was filtered over a Celite bed, and the filtrate was concentrated to get white or off-white solid product, in quantitative yield, which was found to be sufficiently pure enough to use in the next step without further purification.

*4-Aminophenyl 3,4,5-Tributoxybenzoate (**9a**).* $R_f$ = 0.28 (30% EtOAc−hexanes); off-white solid, mp: 112−113 °C. IR (KBr pellet): $\nu_{max}$ in cm$^{-1}$ 3381, 3384, 2958, 2872, 1724, 1625, 1590, 1512, 1432, 1338, 1240, 1192, 1110, 954. $^1$H NMR ($CDCl_3$, 200 MHz): $\delta$ 7.39 (s, 2H, Ar), 6.97 (d, 2H, $J$ = 8.0 Hz, Ar), 6.71 (d, 2H, $J$ = 8.0 Hz, Ar), 4.02−4.08 (m, 6H, 3 × $OCH_2$), 3.66 (brs, 2H, $NH_2$), 0.93−1.88 (m, 21H, 6 × $CH_2$, 3 × $CH_3$). $^{13}$C NMR ($CDCl_3$/$CCl_4$, 100 MHz): 165.4, 152.9, 144.2, 143.1, 142.8, 124.3, 122.3, 115.6, 108.5, 73, 68.8, 32.4, 31.4, 19.3, 19.2, 13.9. MS (FAB+): $m/z$ for $C_{25}H_{35}NO_5$, Calcd: 429.3. Found: 429.9. Anal. Calcd for $C_{25}H_{35}NO_5$: C, 69.90; H, 8.21; N, 3.26. Found: C, 70.21; H, 8.12; N, 3.5.

*4-Aminophenyl 3,4,5-Tris(pentyloxy)benzoate (**9b**).* $R_f$ = 0.29 (30% EtOAc−hexanes); viscous liquid. IR (KBr pellet): $\nu_{max}$ in cm$^{-1}$ 3382, 2960, 2872, 1728, 1622, 1588, 1510, 1433, 1339, 1189, 1117, 950. $^1$H NMR ($CDCl_3$, 200 MHz): $\delta$ 7.39 (s, 2H, Ar), 6.97 (d, 2H, $J$ = 8.8 Hz, Ar), 6.71 (d, 2H, $J$ = 8.6 Hz, Ar), 4.01−4.08 (m, 6H, 3 × $OCH_2$), 3.66 (brs, 2H, $NH_2$), 0.91−1.87 (m, 27H, 9 × $CH_2$, 3 × $CH_3$). $^{13}$C NMR ($CDCl_3$, 100 MHz): 165.5, 152.9, 144.2, 143.2, 142.8, 124.2, 122.3, 115.7, 108.5, 73.5, 69.2, 30.0, 29, 28.22, 28.16, 22.5, 22.4, 14.0. MS (FAB+): $m/z$ for $C_{28}H_{42}NO_5$ [M + 1], Calcd: 472.3. Found: 472.2. Anal. Calcd for $C_{28}H_{41}NO_5$: C, 71.31; H, 8.76; N, 2.97. Found: C, 71.2; H, 8.4; N, 3.1.

*4-Aminophenyl 3,4,5-Tris(hexyloxy)benzoate (**9c**).* $R_f$ = 0.28 (30% EtOAc−hexanes); brown viscous liquid. IR (KBr pellet): $\nu_{max}$ in cm$^{-1}$ 3374, 2931, 2859, 1727, 1624, 1586, 1509, 1430, 1335, 1191, 1114, 952. $^1$H NMR ($CDCl_3$, 200 MHz): $\delta$ 7.39 (s, 2H, Ar), 6.97 (d, 2H, $J$ = 8.0 Hz, Ar), 6.71 (d, 2H, $J$ = 8.0 Hz, Ar), 4.01−4.07 (m, 6H, 3 × $OCH_2$), 3.65 (brs, 2H, $NH_2$), 0.86−1.89 (m, 33H, 12 × $CH_2$, 3 × $CH_3$). $^{13}$C NMR ($CDCl_3$, 100 MHz): 165.6, 152.9, 144.2, 143.1, 142.7, 124.2, 122.3, 115.7, 108.4, 73.5, 69.2, 31.7, 31.5, 30.2, 29.2, 25.7, 25.7, 22.64, 22.58, 14.0. MS (FAB+): $m/z$ for $C_{31}H_{47}NO_5$, Calcd: 513.3. Found: 513.6. Anal. Calcd for $C_{31}H_{47}NO_5$: C, 72.48; H, 9.22; N, 2.73. Found: C, 72.4; H, 9.1; N, 2.9.

*4-Aminophenyl 3,4,5-Tris(heptyloxy)benzoate (**9d**).* $R_f$ = 0.28 (30% EtOAc−hexanes); brown solid, mp: 42−43 °C. IR (KBr pellet): $\nu_{max}$ in cm$^{-1}$ 3624, 3019, 2930, 2858, 1726, 1586, 1510, 1430, 1336, 1215, 1114, 928. $^1$H NMR ($CDCl_3$, 200 MHz): $\delta$ 7.39 (s, 2H, Ar), 6.97 (d, 2H, $J$ = 8.0 Hz, Ar), 6.71 (d, 2H, $J$ = 8.0 Hz, Ar), 4.01−4.07 (m, 6H, 3 × $OCH_2$), 3.65 (brs, 2H, $NH_2$), 0.86−1.89 (m, 39H, 15 × $CH_2$, 3 × $CH_3$). $^{13}$C NMR ($CDCl_3$, 100 MHz): 165.6, 152.9, 144.2, 143.1, 142.7, 124.2, 122.3, 115.7, 108.4, 73.6, 69.2, 31.9, 31.8, 30.3, 29.3, 29.2, 29.0, 26.0, 22.7, 22.6, 14.1. MS (FAB+): $m/z$ for $C_{34}H_{54}NO_5$ [M + 1], Calcd: 556.4. Found: 556.3. Anal. Calcd for $C_{34}H_{53}NO_5$: C, 73.47; H, 9.61; N, 2.52. Found: C, 73.5; H, 9.3; N, 2.6.

*4-Aminophenyl 3,4,5-Tris(octyloxy)benzoate (**9e**).* $R_f$ = 0.27 (30% EtOAc−hexanes); brown solid, mp: 51−52 °C. IR (KBr pellet): $\nu_{max}$ in cm$^{-1}$ 3019, 2929, 2857, 1726, 1586, 1510, 1431, 1336, 1215, 1114, 928. $^1$H NMR ($CDCl_3$, 200 MHz): $\delta$ 7.39 (s, 2H, Ar), 6.99 (d, 2H, $J$ = 8.8 Hz, Ar), 6.75 (d, 2H, $J$ = 8.6 Hz, Ar), 4.0−4.07 (m, 6H, 3 × $OCH_2$), 3.65 (brs, 2H, $NH_2$), 0.85 −1.86 (m, 45H, 18 × $CH_2$, 3 × $CH_3$). $^{13}$C NMR ($CDCl_3$, 100 MHz): 165.6, 152.9, 144.2, 143.1, 142.7, 124.2, 122.3, 115.7, 108.4, 73.5, 69.2, 31.9, 31.8, 30.3, 29.5, 29.32, 29.26, 26.1, 22.6, 14.1. MS (FAB+): $m/z$ for $C_{37}H_{59}NO_5$, Calcd: 597.4. Found: 597.9. Anal. Calcd for $C_{37}H_{59}NO_5$: C, 74.33; H, 9.95; N, 2.34. Found: C, 74.6; H, 9.8; N, 2.5.

*4-Aminophenyl 3,4,5-Tris(decyloxy)benzoate (**9f**).* $R_f$ = 0.28 (30% EtOAc−hexanes); brown solid, mp: 41−42 °C. IR (KBr pellet): $\nu_{max}$ in cm$^{-1}$ 2921, 2851, 1724, 1585, 1510, 1469, 1429, 1336, 1195, 1119, 961. $^1$H NMR ($CDCl_3$, 400 MHz): $\delta$ 7.39 (s, 2H, Ar), 6.97 (d, 2H, $J$ = 12 Hz, Ar), 6.70 (d, 2H, $J$ = 12 Hz, Ar), 4.02−4.07 (m, 6H, 3 × $OCH_2$), 3.67 (bs, 2H, $NH_2$), 0.85 −1.86 (m, 57H, 24 × $CH_2$, 3 × $CH_3$). $^{13}$C NMR ($CDCl_3$, 100 MHz): 165.5, 152.9, 144.2, 143.1, 142.8, 124.2, 122.3, 115.6, 108.5, 73.5, 69.2, 32.0, 31.9, 30.4, 29.7, 29.62, 29.58, 29.5, 29.3, 29.2, 29.1, 26.0, 22.6, 14.1. MS (FAB+): $m/z$ for $C_{43}H_{71}NO_5$, Calcd: 681.5. Found: 681.7. Anal. Calcd for $C_{43}H_{71}NO_5$: C, 75.72; H, 10.49; N, 2.05. Found: C, 75.8; H, 10.6; N, 2.4.

*General Procedure for the Synthesis of the **TLT-n** Series of Compounds.* A round-bottom flask (100 mL capacity) equipped with a magnetic stir bar, reflux condenser, and argon inlet was charged with triformylphloroglucinol (0.168 g, 0.8 mmol, 1 equiv.), 4-aminophenyl 3,4,5-trialkoxybenzoate (5.4 mmol, 6.75 equiv) (**9a−f**), and absolute ethanol (30 mL). The reaction mixture was heated to reflux for 2 h with vigorous stirring. The pale yellow solid separated upon cooling, and the reaction mixture was collected by filtration, repeatedly washed with hot ethanol, and air-dried. The crude product was further purified by repeated recrystallizations in a mixture of absolute ethanol−dichloromethane (9:1) until a constant isotropic phase transition temperature was obtained.

***TLT-4.*** $R_f$ = 0.6 (30% EtOAc−hexanes); yellow solid, yield: 1.2 g (70%). UV−vis: $\lambda_{max}$ = 401.52 nm, $\varepsilon$ = 8.3 × 10$^4$ L mol$^{-1}$ cm$^{-1}$. IR (KBr pellet): $\nu_{max}$ in cm$^{-1}$ 3850, 2957, 2871, 1732, 1619, 1589, 1514, 1455, 1429, 1295, 1183, 1112, 946, 860, 750. $^1$H NMR ($CDCl_3$, 400 MHz): $\delta$ 13.42−13.49 (m, =CNH), 13.06 (d, $J$ = 13.2 Hz, =CNH), 13.04 (d, $J$ = 13.2 Hz, =CNH) − these resonances are due to three amine protons, 8.71−8.83 (m, 3H, =CHN), 7.25−7.41 (m, 18H, Ar), 4.04−4.09 (m, 18H, 9 × $OCH_2$), 0.97−1.86 (m, 63H, 18 × $CH_2$, 9 × $CH_3$). $^{13}$C NMR ($CDCl_3$, 100 MHz): 188.3, 185.5, 182.4, 165, 153, 150.3, 149.8, 149.4, 148.7, 148.61, 148.57, 143.2, 136.8, 123.5, 123.4, 118.6, 118.5, 108.6, 107.1, 107, 106.8, 73.2, 69.0, 32.3, 31.3, 19.2, 19.1, 13.1; MS (FAB+): $m/z$ for $C_{84}H_{106}N_3O_{18}$ [M + 1], Calcd: 1444.75. Found: 1445.8. Anal. Calcd for $C_{84}H_{105}N_3O_{18}$: C, 69.83; H, 7.33; N, 2.91. Found: C, 70.2; H, 7.6; N, 3.

***TLT-5.*** $R_f$ = 0.6 (30% EtOAc−hexanes); yellow solid, yield: 1.3 g (70%). UV−vis: $\lambda_{max}$ = 403.45 nm, $\varepsilon$ = 7.4 × 10$^4$ L mol$^{-1}$ cm$^{-1}$. IR (KBr pellet): $\nu_{max}$ in cm$^{-1}$ 3850, 2955, 2870, 1735, 1620, 1590, 1513, 1457, 1430, 1295, 1184, 1112, 990, 857, 751. $^1$H NMR ($CDCl_3$, 400 MHz): $\delta$ 13.42−13.49 (m, =CNH), 13.06 (d, $J$ = 13.2 Hz, =CNH), 13.04 (d, $J$ = 13.2 Hz, =CNH) − these resonances are due to three amine protons, 8.71−8.82 (m, 3H, =CHN), 7.25−7.41 (m, 18H, Ar), 4.04−4.09 (m, 18H, 9 × $OCH_2$), 1.36−1.88 (m, 54H, 27 × $CH_2$), 0.93


dx.doi.org/10.1021/jo302332u | J. Org. Chem. 2013, 78, 527−544

(t, $J$ = 7.2 Hz, 27H, 9 × $CH_3$). $^{13}C$ NMR ($CDCl_3$, 100 MHz): 188.3, 185.5, 182.4, 165.0, 153.0, 150.3, 149.8, 149.4, 148.62, 148.58, 143.2, 136.8, 123.5, 123.4, 118.6, 118.64, 108.55, 107.1, 107.0, 106.8, 73.6, 69.3, 30.0, 29.0, 28.23, 28.17, 22.5, 22.4, 14.1. MS (FAB+): $m/z$ for $C_{93}H_{124}N_3O_{18}$ [M + 1], Calcd: 1570.9. Found: 1571.6. Anal. Calcd for $C_{93}H_{123}N_3O_{18}$: C, 71.1; H, 7.89; N, 2.67. Found: C, 71.2; H, 7.7; N, 2.8.

***TLT-6***. $R_f$ = 0.6 (30% EtOAc−hexanes); yellow solid, yield: 1.4 g (67%). UV−vis: $\lambda_{max}$ = 401.1 nm, $\varepsilon = 9.8 \times 10^4$ L mol$^{-1}$ cm$^{-1}$. IR (KBr pellet): $\nu_{max}$ in cm$^{-1}$ 3743, 2931, 2859, 1733, 1621, 1590, 1514, 1456, 1429, 1295, 1184, 1114, 962, 859, 752. $^1H$ NMR ($CDCl_3$, 400 MHz): $\delta$ 13.42−13.49 (m, =CNH), 13.06 (d, $J$ = 13.2 Hz, =CNH), 13.04 (d, $J$ = 13.2 Hz, =CNH) − these resonances are due to three amine protons, 8.71−8.83 (m, 3H, =CHN), 7.25−7.41 (m, 18H, Ar), 4.04−4.09 (m, 18H, 9 × $OCH_2$), 1.31−1.87 (m, 72H, 36 × $CH_2$), 0.93 (t, $J$ = 6.8 Hz, 27H, 9 × $CH_3$). $^{13}C$ NMR ($CDCl_3$, 100 MHz): 188.3, 185.5, 182.4, 165.0, 153.0, 150.3, 149.8, 149.4, 148.62, 148.57, 143.2, 136.8, 123.5, 123.4, 118.6, 118.5, 108.6, 107.1, 107.0, 106.8, 73.6, 69.3, 31.7, 31.5, 30.3, 29.3, 25.73, 25.68, 22.7, 22.6, 14.1. MS (FAB+): $m/z$ for $C_{102}H_{142}N_3O_{18}$ [M + 1], Calcd: 1697.0. Found: 1697.0. Anal. Calcd for $C_{102}H_{141}N_3O_{18}$: C, 72.18; H, 8.37; N, 2.48. Found: C, 72.5; H, 8.6; N, 2.6.

***TLT-7***. $R_f$ = 0.55 (30% EtOAc−hexanes); yellow solid, yield: 1.5 g (65%). UV−vis: $\lambda_{max}$ = 401.52 nm, $\varepsilon = 11.4 \times 10^4$ L mol$^{-1}$ cm$^{-1}$. IR (KBr pellet): $\nu_{max}$ in cm$^{-1}$ 3743, 2926, 2855, 1735, 1621, 1590, 1513, 1457, 1429, 1294, 1183, 1114, 860, 751. $^1H$ NMR ($CDCl_3$, 400 MHz): $\delta$ 13.43−13.50 (m, =CNH), 13.06 (d, $J$ = 13.2 Hz, =CNH), 13.04 (d, $J$ = 12.8 Hz, =CNH) − these resonances are due to three amine protons, 8.71−8.84 (m, 3H, =CHN), 7.26−7.41 (m, 18H, Ar), 4.04−4.09 (m, 18H, 9 × $OCH_2$), 1.26−1.88 (m, 90H, 45 × $CH_2$,), 0.93 (m, 27H, 9 × $CH_3$). $^{13}C$ NMR ($CDCl_3$, 100 MHz): 188.3, 185.5, 182.5, 165, 153, 150.3, 149.8, 150, 149, 148.63, 148.58, 143.2, 136.8, 123.5, 123.4, 118.64, 118.55, 108.6, 107.1, 107, 106.8, 73.6, 69.3, 31.9, 31.8, 30.3, 29.3, 29.2, 29.0, 26.0, 22.7, 22.6, 14.1. MS (FAB+): $m/z$ for $C_{111}H_{160}N_3O_{18}$ [M + 1], Calcd: 1823.2. Found: 1823. Anal. Calcd for $C_{111}H_{159}N_3O_{18}$: C, 73.11; H, 8.79; N, 2.3. Found: C, 73.4; H, 9.0; N, 2.4.

***TLT-8***. $R_f$ = 0.55 (30% EtOAc−hexanes); yellow solid, yield: 1.6 g (71%). UV−vis: $\lambda_{max}$ = 401.4 nm, $\varepsilon = 26.6 \times 10^4$ L mol$^{-1}$ cm$^{-1}$. IR (KBr pellet): $\nu_{max}$ in cm$^{-1}$ 3745, 2926, 1735, 1624, 1590, 1513, 1457, 1430, 1296, 1183, 1116, 860, 752. $^1H$ NMR ($CDCl_3$, 400 MHz): $\delta$ 13.43−13.50 (m, =CNH), 12.9−13.06 (m, =CNH) − these resonances are due to three amine protons, 8.72−8.84 (m, 3H, =CHN), 7.26−7.41 (m, 18H, Ar), 4.04−4.09 (m, 18H, 9 × $OCH_2$), 1.29−1.87 (m, 108H, 54 × $CH_2$,), 0.93 (m, 27H, 9 × $CH_3$). $^{13}C$ NMR ($CDCl_3$, 100 MHz): 188.3, 185.5, 182.4, 165.0, 153.0, 150.3, 149.8, 149.5, 148.63, 148.58, 143.3, 136.8, 123.5, 123.4, 118.64, 118.55, 108.6, 107, 106.8, 73.6, 69.3, 31.9, 31.8, 30.3, 29.5, 29.33, 29.30, 29.26, 26.1, 26.0, 22.7, 14.1. MS (FAB+): $m/z$ for $C_{120}H_{178}N_3O_{18}$ [M + 1], Calcd: 1949.3. Found: 1950.0. Anal. Calcd for $C_{120}H_{177}N_3O_{18}$: C, 73.92; H, 9.15; N, 2.4. Found: C, 73.7; H, 9.2; N, 2.3.

***TLT-10***. $R_f$ = 0.55 (30% EtOAc−hexanes); yellow solid, yield: 1.8 g (69%). UV−vis: $\lambda_{max}$ = 401.58 nm, $\varepsilon = 8.5 \times 10^4$ L mol$^{-1}$ cm$^{-1}$. IR (KBr pellet): $\nu_{max}$ in cm$^{-1}$ 3450, 2923, 2852, 1735, 1622, 1590, 1514, 1456, 1430, 1296, 1185, 1116, 860, 750. $^1H$ NMR ($CDCl_3$, 400 MHz): $\delta$ 13.42−13.49 (m, =CNH), 13.06 (d, $J$ = 13.2 Hz, =CNH), 13.04 (d, $J$ = 13.2 Hz, =CNH) − these resonances are due to three amine protons, 8.71−8.83 (m, 3H, =CHN), 7.26 −7.41 (m, 18H, Ar), 4.03−4.09 (m, 18H, 9 × $OCH_2$), 1.28 −1.89 (m, 144H, 72 × $CH_2$,), 0.93 (m, 27H, 9 × $CH_3$). $^{13}C$ NMR ($CDCl_3$, 100 MHz): 188.3, 185.5, 182.4, 164.9, 153.0, 150.2, 149.8, 149.4, 148.7, 148.61, 148.57, 143.2, 136.8, 123.5, 123.3, 118.6, 118.5, 108.6, 107.1, 107.0, 106.8, 74.0, 69.3, 31.9, 30.3, 29.71, 29.65, 29.61, 29.56, 29.4, 29.3, 28.9, 26.1, 22.7, 14.1. Anal. Calcd for $C_{138}H_{213}N_3O_{18}$: C, 75.27; H, 9.75; N, 1.91. Found: C, 75.3; H, 10.2; N, 1.9.

## ■ ASSOCIATED CONTENT

### Supporting Information

Copies of $^1H$ and $^{13}C$ NMR spectra of all new compounds. This material is available free of charge via the Internet at http://pubs.acs.org.

## ■ AUTHOR INFORMATION


### Corresponding Author

*Phone: 91-80-2838 1119; fax: 91-80-28382044; e-mail: Yelamaggad@gmail.com.

### Present Address

†Department of Chemistry, Indian Institute of Technology Guwahati, Guwahati-781039, Assam, India.


### Notes

The authors declare no competing financial interest.

## ■ ACKNOWLEDGMENTS

We sincerely thank Department of Science and Technology (DST), New Delhi, Government of India, for financial support of this work through SERC project no. SR/S1//OC-06/2007. We also thank Mr. V. Swami for his assistance in the preparation and characterization of some precursors. U.S.H. thanks DST for the fellowship under WOS-A scheme.

## ■ REFERENCES


(1) (a) Coropceanu, V.; Cornil, J.; da Silva Filho, D. A.; Olivier, Y.; Silbey, R.; Brédas, J.-L. *Chem. Rev.* **2007**, *107*, 926−952. (b) He, G. S.; Tan, L. S.; Zheng, Q. D.; Prasad, P. N. *Chem. Rev.* **2008**, *108*, 1245−1330. (c) Cheng, Y.-J.; Yang, S.-H.; Hsu, C.-S. *Chem. Rev.* **2009**, *109*, 5868−5923. (d) Grimsdale, A. C.; Chan, K. L.; Martin, R. E.; Jokisz, P. G.; Holmes, A. B. *Chem. Rev.* **2009**, *109*, 897−1091. (e) Weber, H. B.; Reichert, J.; Weigend, F.; Ochs, R.; Beckmann, D.; Mayor, M.; Ahlrichs, R.; von Lohneysen, H. *Chem. Phys.* **2002**, *281*, 113−125.

(2) (a) Pope, M; Swenberg, C. *Electronic Processes in Organic Crystals and Polymers*, 2nd ed.; Oxford University Press: London, 1999. (b) Klauk, H. *Organic Electronics: Materials, Manufacturing and Applications*; Wiley-VCH Verlag GmbH: Weinheim, Germany, 2006. (c) Sundar, V. C.; Zaumseil, J.; Podzorov, V.; Someya, T.; Gershenson, M. E.; Rogers, J. A. *Science* **2004**, *303*, 1644−1646. (d) Podzorov, V.; Menard, E.; Borissov, A.; Kiryukhin, V.; Rogers, J. A.; Gershenson, M. E. *Phys. Rev. Lett.* **2004**, *93*, 086602. (e) Tang, Q.; Li, H.; He, M.; Hu, W.; Liu, C.; Chen, K.; Wang, C.; Liu, Y.; Zhu, D. *Adv. Mater.* **2006**, *18*, 65−68.

(3) (a) LeBlanc, O. H., Jr. *J. Chem. Phys.* **1960**, *33*, 626. (b) Kepler, R. G. *Phys. Rev.* **1960**, *119*, 1226−1229. (c) Mohwald, H.; Haarer, D.; Castro, G. *Chem. Phys. Lett.* **1975**, *32*, 433−437. (d) Karl, N.; Ziegler, J. *Chem. Phys. Lett.* **1975**, *32*, 438−442.

(4) For recent reviews on discotic liquid crystals see (a) Sergeyev, S.; Pisula, W.; Geerts, Y. H. *Chem. Soc. Rev.* **2007**, *36*, 1902−1929. (b) Laschat, S.; Baro, A.; Steinke, N.; Giesselmann, F.; Hagele, C.; Scalia, G.; Judele, R.; Kapatsina, E.; Sauer, S.; Schreivogel, A.; Tosoni, M. *Angew. Chem., Int. Ed.* **2007**, *46*, 4832−4837. (c) Pisula, W.; Zorn, M.; Chang, J. Y.; Müllen, K.; Zentel, R. *Macromol. Rapid Commun.* **2009**, *30*, 1179−1202. (d) Kumar, S. *Chemistry of Discotic Liquid Crystals: From Monomers to Polymers*; CRC Press: Boca Raton, FL, 2010. (e) Kaafarani, B. R. *Chem. Mater.* **2011**, *23*, 378−396.

(5) Chandrasekhar, S.; Sadashiva, B. K.; Suresh, K. A. *Pramana* **1977**, *9*, 471−480.

(6) (a) Adam, D.; Schuhmacher, P.; Simmerer, J.; Haussling, L.; Siemensmeyer, K.; Etzbachi, K. H.; Ringsdorf, H.; Haarer, D. *Nature* **1994**, *371*, 141−143. (b) Percec, V.; Glodde, M.; Bera, T. K.; Miura, Y.; Shiyanovskaya, I.; Singer, K. D.; Balagurusamy, V. S.; Heiney, P. A.; Schnell, I.; Rapp, A.; Spiess, H. W.; Hudson, S. D.; Duan, H. *Nature* **2002**, *419*, 384−387.

(7) Li, Q. *Self-Organized Organic Semiconductors: From Materials to Device Applications*; John Wiley & Sons: New York, 2011.

(8) (a) Van De Craats, A. M.; Warman, J. M.; Fechtenkotter, A.; Brand, J. D.; Harbison, M. A.; Müllen, K. *Adv. Mater.* **1999**, *11*, 1469−1472. (b) Debije, M. G.; Piris, J.; De Haas, M. P.; Warman, J. M.; Tomović, Z.; Simpson, C. D.; Watson, M. D.; Müllen, K. *J. Am. Chem. Soc.* **2004**, *126*, 4641−4645. (c) An, Z.; Yu, J.; Jones, S. C.; Barlow, S.; Yoo, S.; Domercq, B.; Prins, P.; Siebbeles, L. D. A.; Kippelen, B.; Marder, S. R. *Adv. Mater.* **2005**, *17*, 2580−2583.
(9) (a) Yelamaggad, C. V.; Achalkumar, A. S.; Rao, D. S. S.; Prasad, S. K. *J. Am. Chem. Soc.* **2004**, *126*, 6506−6507. (b) Yelamaggad, C. V.; Achalkumar, A. S. *Tetrahedron Lett.* **2006**, *47*, 7071−7075. (c) Yelamaggad, C. V.; Achalkumar, A. S.; Rao, D. S. S.; Prasad, S. K. *J. Org. Chem.* **2007**, *72*, 8308−8318. (d) Yelamaggad, C. V.; Achalkumar, A. S.; Rao, D. S. S.; Prasad, S. K. *J. Org. Chem.* **2009**, *74*, 3168−3171. (e) Yelamaggad, C. V.; Achalkumar, A. S. *Tetrahedron Lett.* **2012**, *53*, 7108−7112.
(10) Yelamaggad, C. V.; Rashmi Prabhu, D. S. S.; Prasad, S. K. *Tetrahedron Lett.* **2010**, *51*, 4579−4583.
(11) (a) Chong, J. H.; Sauer, M.; Patrick, B. O.; MacLachlan, M. J. *Org. Lett.* **2003**, *5*, 3823−3826. (b) Sauer, M.; Yeung, C.; Chong, J. H.; Patrick, B. O.; MacLachlan, M. J. *J. Org. Chem.* **2006**, *71*, 775−788.
(12) (a) Riddle, J. A.; Bollinger, J. C.; Lee, D. *Angew. Chem., Int. Ed.* **2005**, *44*, 6689−6693. (b) Riddle, J. A.; Lathrop, S. P.; Bollinger, J. C.; Lee, D. *J. Am. Chem. Soc.* **2006**, *128*, 10986−10987. (c) Jiang, X.; Bollinger, J. C.; Lee, D. *J. Am. Chem. Soc.* **2006**, *128*, 11732−11733.
(13) For recent reviews on star-shaped mesogens, the hekates, see (a) Lehman, M. *Chem.—Eur. J.* **2009**, *15*, 3638−3651. (b) Lehman, M. *Top Curr. Sci.* **2012**, *318*, 193−224.
(14) (a) Pesak, D. J.; Moore, J. S. *Angew. Chem., Int. Ed. Engl.* **1997**, *36*, 1636−1639. (b) Kim, B. G.; Kim, S.; Park, S. Y. *Tetrahedron Lett.* **2001**, *42*, 2697−2699. (c) Tanabe, K.; Yasuda, T.; Kato, T. *Chem. Lett.* **2008**, *37*, 1208−1209. (d) Tomovic, Z.; van Dongen, J.; George, S. J.; Xu, H.; Pisula, W.; Leclere, P.; Smulders, M. M. J.; De Feyter, S.; Meijer, E. W.; Schenning, A. P. H. J. *J. Am. Chem. Soc.* **2007**, *129*, 16190−16196. (e) Luo, J.; Zhao, B.; Chan, H. S. O.; Chi, C. *J. Mater. Chem.* **2010**, *20*, 1932−1941. (f) Kanibolotsky, A. L.; Perepichka, I. F.; Skabara, P. J. *Chem. Soc. Rev.* **2010**, *39*, 2695−2728.
(15) Dambal, H. K.; Yelamaggad, C. V. *Tetrahedron Lett.* **2012**, *53*, 186−190.
(16) Lehmann, M.; Jahr, M.; Gutmann, J. *J. Mater. Chem.* **2008**, *18*, 2995−3003.
(17) Palmans, A. R. A.; Vekemans, J. A. J. M.; Hikmet, R. A.; Fischer, H.; Meijer, W. E. *Adv. Mater.* **1998**, *10*, 873−876.
(18) Lehmann, M.; Jahr, M.; Grozema, F. C.; Abellon, R. D.; Siebbeles, L. D. A.; Muller, M. *Adv. Mater.* **2008**, *20*, 4414−4418.
(19) (a) Omenat, A.; Barber, J.; Serrano, J.-L.; Houbrechts, S.; Persoons, A. *Adv. Mater.* **1999**, *11*, 1292−1295. (b) Cho, B. R.; Chajara, K.; Oh, H. J.; Son, K. H.; Jeon, S.-J. *Org. Lett.* **2002**, *4*, 1703−1706. (c) Meier, H. *Angew. Chem., Int. Ed.* **2005**, *44*, 2482−2506.
(20) Ryu, S. Y.; Kim, S.; Seo, J.; Kim, Y.-W.; Kwon, O.-H.; Jang, D.-J.; Park, S. Y. *Chem. Commun.* **2004**, 70−71.
(21) (a) Meier, H.; Lehmann, M. *Angew. Chem., Int. Ed.* **1998**, *37*, 643−645. (b) Meier, H.; Lehmann, M.; Holst, H. C.; Schwçppe, D. *Tetrahedron* **2004**, *60*, 6881−6888. (c) Lehmann, M.; Kohn, C.; Meier, H.; Renker, S.; Oehlhof, A. *J. Mater. Chem.* **2006**, *16*, 441−451.
(22) Ponomarenko, S. A.; Kirchmeyer, S.; Elschner, A.; Huisman, B.-H.; Karbach, A.; Drechsler, D. *Adv. Funct. Mater.* **2003**, *13*, 591−596.
(23) (a) Mukkamala, R.; Burns, C. L., Jr.; Catchings, R. M., III; Weiss, R. G. *J. Am. Chem. Soc.* **1996**, *118*, 9498−9508. (b) Nguyen, H. T.; Destrade, C.; Malthete, J. *Liq. Cryst.* **1990**, *8*, 797−811. (c) Chen, H.-B.; Yin, J.; Wang, Y.; Pei, J. *Org. Lett.* **2008**, *10*, 3113−3116. (d) Eisenbraun, E. J. *Org. Synth.* **1973**, *5*, 310.
(24) Maruyama, S.; Sato, K.; Iwahashi, H. *Chem. Lett.* **2010**, *39*, 714−716.
(25) (a) Judele, R.; Laschat, S.; Baro, A.; Nimtz, M. *Tetrahedron* **2006**, *62*, 9681−9687. (b) Marquet, J.; Moreno-Manas, M.; Vallribera, A.; Virgili, A.; Bertran, J.; Gonzalez-Lafont, A.; Lluch, J. M. *Tetrahedron* **1987**, *43*, 351−360. (c) Schultz, A.; Diele, S.; Laschat, S.; Nimtz, M. *Adv. Funct. Mater.* **2001**, *11*, 441−446. (d) Ungar, G.; Abramic, D.; Percec, V.; Heck, J. A. *Liq. Cryst.* **1996**, *21*, 73−86. (e) Majumdar, K. C.; Ansary, I.; Roy, B. *Mol. Cryst. Liq. Cryst.* **2010**, *518*, 160−167. (f) Terazzi, E.; Torelli, S.; Bernardinelli, G.; Rivera, J.-P.; Benech, J.-M.; Bourgogne, C.; Donnio, B.; Guillon, D.; Imbert, D.; Buenzli, J.-C. G.; Pinto, A; Jeannerat, D.; Piguet, C. *J. Am. Chem. Soc.* **2005**, *127*, 888−903.
(26) Ito, S.; Ando, M.; Nomura, A.; Morita, N.; Kabuto, C.; Mukai, H.; Ohta, K.; Kawakami, J.; Yoshizawa, A.; Tajiri, A. *J. Org. Chem.* **2005**, *70*, 3939−3949.
(27) (a) Hayer, A.; de Halleux, V.; Kohler, A.; El-Garoughy, A.; Meijer, E. W.; Barbera, J.; Tant, J.; Levin, J.; Lehmann, M.; Gierschner, J.; Cornil, J.; Geerts, Y. H. *J. Phys. Chem. B* **2006**, *110*, 7653−7659. (b) Barbera, J.; Gimenez, R.; Serrano, J. L. *Chem. Mater.* **2000**, *12*, 481−489 (and references cited therein). (c) Alavarez, L.; Barbera, J.; Puig, L.; Romero, P.; Serrano, J. L.; Sierra, T. *J. Mater. Chem.* **2006**, *16*, 3768−3773. (d) Carfagna, C.; Roviello, A.; Sirigu, A. *Mol. Cryst. Liq. Cryst.* **1985**, *122*, 151−160. (e) Gramsbergen, E. F.; Hoving, H. J.; de Jeu, W. H.; Praefcke, K.; Kohne, B. *Liq. Cryst.* **1986**, *1*, 397−400. (f) Metersdorf, H.; Ringsdorf, H. *Liq. Cryst.* **1989**, *5*, 1757−1772. (g) Zeng, H.; Carroll, P. J.; Swager, T. M. *Liq. Cryst.* **1993**, *14*, 1421−1429. (h) Van Nostrum, C. F.; Bosman, A. W.; Gelinck, G. H.; Schouten, P. G.; Warman, J. M.; Kentgens, A. P. M.; Devillers, M. A. C.; Meijerink, A.; Picken, S. J.; Sohling, U.; Schouten, A.-J.; Nolte, R. J. M. *Chem.—Eur. J.* **1995**, *1*, 171−182 (and references therein). (i) Serrano, J. L.; Sierra, T. *Chem.—Eur. J.* **2000**, *6*, 759−766.
(28) (a) Destrade, C.; Foucher, P.; Gasparoux, H.; Nguyen Huu, T.; Levelut, A. M.; Malthete, J. *Mol. Cryst. Liq. Cryst.* **1984**, *106*, 121−146. (b) Morale, F.; Date, R. W.; Guillon, D.; Bruce, D. W.; Finn, R. L.; Wilson, C.; Blake, A. J.; Schröder, M.; Donnio, B. *Chem.—Eur. J.* **2003**, *9*, 2484−2501. (c) Choi, J.-W.; Han, J.-H.; Ryu, M.-H.; Cho, B.-K. *Bull. Korean Chem. Soc.* **2011**, *32*, 781−782. (d) Yelamaggad, C. V.; Shanker, G.; Rao, R. V.; Shankar Rao, D. S.; Prasad, S. K.; Babu, V. V. S. *Chem.—Eur. J.* **2008**, *14*, 10462−10471.
(29) Beer, A.; Scherowsky, G.; Owen, H.; Coles, H. *Liq. Cryst.* **1995**, *19*, 565−572 (and references therein).
(30) Christ, T.; Glusen, B.; Greiner, A.; Kettner, A.; Sander, R.; Stumpflen, V.; Tsukruk, V.; Wendorff, J. H. *Adv. Mater.* **1997**, *9*, 48−52.
(31) Bernard, V. *Molecular Fluorescence: Principles and Applications*; Wiley-VCH: Weinheim, Germany, 2001.
(32) (a) Würthner, F.; Thalacker, C.; Diele, S.; Tschierske., C. *Chem.—Eur. J.* **2001**, *7*, 2245−2253. (b) Langhals, H.; Ismael, R. *Eur. J. Org. Chem.* **1998**, 1915−1917. (c) Valdes-Aguilera, O.; Neckers, D. C. *Acc. Chem. Res.* **1989**, *22*, 171−177. (d) Davis, R.; Rath, N. P.; Das, S. *Chem. Commun.* **2004**, 74−75. (e) Davis, R.; Abraham, S.; Rath, N. P.; Das, S. *New J. Chem.* **2004**, *28*, 1368−1372. (f) Abraham, S.; Mallia, A. V.; Ratheesh, K. V.; Tamaoki, N.; Das, S. *J. Am. Chem. Soc.* **2006**, *128*, 7692−7698.
(33) Levitsky, I. A.; Kishikawa, K.; Eichhorn, S. H.; Swager., T. M. *J. Am. Chem. Soc.* **2000**, *122* (11), 2474−2479.
(34) (a) Chi, Z.; Zhang, X.; Xu, B.; Zhou, X.; Ma, C.; Zhang, Y.; Liu, S.; Xu, J. *Chem. Soc. Rev.* **2012**, *41*, 3878−3896 (and references cited therein). (b) Pschirer, N. G.; Vaughn, M. E.; Dong, Y. B.; zur Loye, H.-C.; Bunz, U. H. F. *Chem. Commun.* **2000**, 85−86. (c) Halkyard, C. E.; Rampey, M. E.; Kloppenburg, L.; Studer-Martinez, S. L.; Bunz, U. H. F. *Macromolecules* **1998**, *31*, 8655−8659. (d) Ofer, D.; Swager, T. M.; Wrighton, M. S. *Chem. Mater.* **1995**, *7*, 418−425. (e) Zhou, Q.; Swager, T. M. *J. Am. Chem. Soc.* **1995**, *117*, 12593−12602. (f) Weder, C.; Wrighton, M. S. *Macromolecules* **1996**, *29*, 5157−5165.